Inorganic Chemistry

Article

pubs.acs.org/IC

Role of Single-Ion Anisotropy and Magnetic Exchange Interactions in Suppressing Zero-Field Tunnelling in {3d-4f} Single Molecule Magnets

Tulika Gupta, Mohammad Faizan Beg, and Gopalan Rajaraman*

Department of Chemistry, Indian Institute of Technology Bombay, Mumbai 400076, India

Supporting Information

ABSTRACT: Extensive ab initio CASSCF/RASSI-SO/SINGLE_ANISO/POLY_ANISO calculations have been undertaken on eight structurally similar previously synthesized $[Cu^{II}(L)(C_3H_6O)Ln^{III}(NO_3)_3]$ (Ln = Dy (**1**), Tb (**3**), Ho (**5**), and Er (**7**)) and $[V^{IV}O(L)(C_3H_6O)Ln^{III}(NO_3)_3]$ (Ln = Dy (**2**), Tb (**4**), Ho (**6**), and Er (**8**)) (here H_2L = *N*,*N*′-bis(3-methoxysalicylidene)-1,3-diamino-2,2-dimethylpropane) complexes (crystal structures reported earlier). Our estimated exchange interactions (J) using the Lines model for complexes **1**−**8** (1.55 cm^{-1}, 0.15 cm^{-1}, 5.30 cm^{-1}, 0.06 cm^{-1}, 1.05 cm^{-1}, −0.18 cm^{-1}, 0.24 cm^{-1}, and −0.02 cm^{-1} for complexes **1**−**8** respectively) match well with the experimental values (HE-EPR and pulse magnetization technique) reported earlier and offer confidence in the methodology employed. We have established the mechanism of magnetic coupling for this series to rationalize the observation that LnCu complexes are strongly coupled compared to LnV complexes. Besides, the results procured based on the BS-DFT method imply a crucial role of overlap between the 3d and 4f orbitals, the formally empty 5d/6s/6p orbitals of Ln^{III} ion in the exchange coupling mechanism. To probe the origin/absence of magnetization relaxation observed in these complexes **1**−**8**, both the single-ion and the exchange anisotropy are analyzed. Our calculations reveal that stronger exchange interaction quenches the quantum tunnelling of magnetization behavior in these complexes; however, for LnV complexes the exchange interaction was too small to offer a large blockade barrier. In the quest to obtain a stronger exchange interaction, we have assessed several models and have developed a magneto-structural correlation. An antagonizing behavior between the J_{CuDy} and U_{cal} values are noted for the Dy−O−O−Cu dihedral angle correlation developed on complex **1**. This highlights the subtle nature of the magnetic anisotropy in this class of complexes and postulates that both the single-ion anisotropy and the exchange interaction are needed to be targeted simultaneously to achieve a new generation {3d-4f} single molecule magnets (SMM).

1. INTRODUCTION

Single molecule magnets (SMMs)[1] are an inquisitive area of research as diversified applications such as spin valves, transistors, q-bits, molecular refrigerants, ultrahigh density information storage devices, ultrafast information processing devices, and molecular spintronics, etc. have been proposed for this class of molecules.[2] SMMs show slow relaxation of magnetization below a certain blocking temperature and hence retain magnetic properties for longer periods of time at the molecular level. This slow relaxation can be ascribed to the effective barrier ($U_{eff} \approx |D|S^2$) for the reversal of magnetization, and this can be considered as the energy required to transform the SMM into a usual paramagnet. Uniaxial magnetic anisotropy (D; axial zero-field splitting parameter) and ground states with large spin (S) are considered as major criteria for designing a SMM based on transition metal ions. Additionally, working blocking temperature (T_B; temperature at which divergence between the field-cooled and the zero-field cooled curves are observed) where SMMs are functional must be improved to room temperature values,[3] as SMMs reported until now function only at liquid helium temperatures. The primary challenge in this area is the magnetic anisotropy which decreases tremendously when the cluster size or spin ground state increases.[4,5] As the anisotropy being the primary criteria and this can be fine-tuned easily for mononuclear complexes, several low-coordinate mononuclear transition metal complexes with attractive barrier heights have been reported.[6] Although these low-coordinate transition metal complexes are attractive, they are often difficult to synthesize and are unstable in ambient conditions.[7] These observations triggered the search for metal ion, possessing large inherent anisotropy, and lanthanides are found to be the obvious solution to these issues.

Lanthanide based complexes play a pivotal role in the area of SMMs.[8−10] The ground spin−orbital manifold J in lanthanide complexes is similar to the spin ground state S in transition metal clusters, while the crystal field splitting of J multiplets is comparable to the axial zero-field splitting parameter in transition metal complexes.[11] This promotes the use of lanthanides in molecular magnetism as the ground state is essentially defined by the $(2J + 1)$ term {the multiplicity of the ground J level}, by fabricating the ligand field surrounding

Received: July 28, 2016
Published: October 13, 2016

DOI: 10.1021/acs.inorgchem.6b01831
Inorg. Chem. 2016, 55, 11201−11215

Scheme 1. Schematic Representation of Crystallographic Geometries (a) $[Cu^{II}(L)(C_3H_6O)Ln^{III}(NO_3)_3]$ {Ln = Dy (1), Tb (3), Ho (5), and Er (7)} and (b) $[V^{IV}O(L)(C_3H_6O)Ln^{III}(NO_3)_3]$ {Ln = Dy (2), Tb (4), Ho (6) and Er (8)}

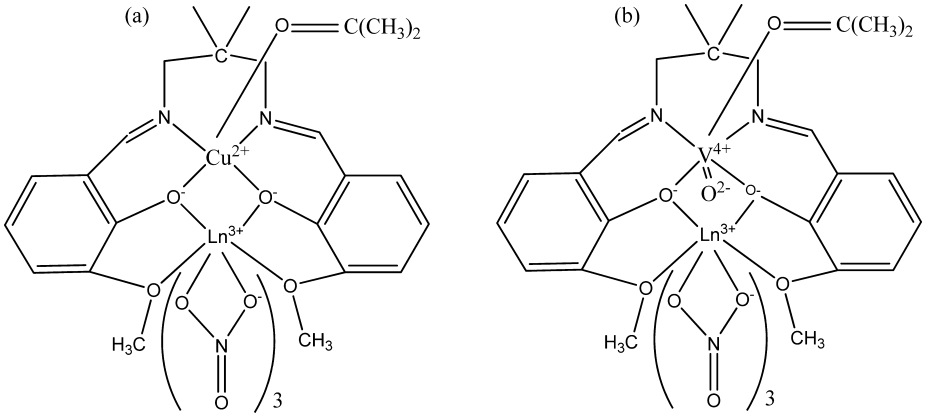

metal, we could achieve extremely huge magnetic anisotropy for magnetization reversal. This is exemplified by the recent discovery that a seven-coordinate Dy^{III} complex is found to exhibit a hysteresis loop up to 30 K.[51]

One of the major disadvantages of lanthanides lies in mediating very weak exchange interactions, and this opens up many relaxation pathways rendering the U_{eff} ineffective for magnetization blockade.[3b,12,8f,13] Particularly the QTM process is very rapid in many lanthanide complexes, and hence it is very rare to observe a magnetic hysteresis with a large coercive field in lanthanide based SMMs.[14−16]An efficient strategy to quench the QTM is to promote strong magnetic exchange interaction, and this can be achieved using either radical ligands[3b,17] or a 3d metal ion. There is a large body of literature available to pinpoint exchange interactions between the 3d and 4f ions as the impetus for quenching of QTM behavior, and this concept has been exploited to synthesize several {3d-4f} polynuclear complexes possessing attractive barrier heights and blocking temperatures.[3d,18] As the 3d metal ions can also offer anisotropy, a correct choice of the metal ions can lead to enhancement of the magnetic anisotropy and larger U_{eff} values. For these reasons, efforts in synthesizing novel {3d-4f}[14,18a,8b,19,20] complexes are of paramount importance in achieving a new generation SMMs. However, because of the complexity involved in factoring out all of the contributions toward magnetic anisotropy in polynuclear complexes, interpreting the magnetic properties of {3d-4f} complexes poses a challenge.

Despite the fact that exchange interactions render such a crucial contribution in quenching QTM behavior, there are only a few reports where these interactions are accurately estimated using experimental means.[21,50] On the same note, though experimental techniques,[48] such as inelastic neuron scattering (INS)[22] and multifrequency high-field EPR[23] have been used to probe the magnetic anisotropy in exchange coupled systems, none of them suffice to resolve the directions of the local magnetic anisotropy axis accurately. Rapid progress in quantum chemistry methods and enhanced computational resources remedy such issues through the use of fully ab initio calculations.[3a,d,13a,15,18,25,28,29,35,24,50a,53] They have been proven valuable in a profound understanding of the complicated nature of the magnetic properties of anisotropic systems. The exchange interactions in anisotropic {3d-4f} systems could be extracted within the Lines model employing anisotropic contributions, energies, and wave functions from ab initio calculations.[18a,19d,g,h,25] In this regard, the report of eight complexes covering the four lanthanide metal ions {Dy^{III}, Tb^{III}, Er^{III}, and Ho^{III}} with the variation of Cu^{II} and V^{IV} metals reported by Ishida and co-workers gain importance as these complexes are characterized by high-field high frequency electron paramagnetic resonance (HF-EPR) techniques for the first time.[21b] Using HF-EPR and pulsed-field magnetization techniques, the exchange coupling parameter for the aforementioned eight complexes are estimated. As anisotropy of the systems are very high, this demands study in the frequency range of 95−400 GHz at 4.2 K, revealing the scarcity of such a study.[21b]

In our present work, we aim to employ an ab initio (CASSCF+RASSI-SO+SINGLE_ANISO) method to model the magnetic properties of eight complexes having the molecular formula of $[Cu^{II}(L)(C_3H_6O)Ln^{III}(NO_3)_3]$ {Ln = Dy (**1**), Tb (**3**), Ho (**5**), and Er (**7**)} and $[V^{IV}O(L)(C_3H_6O)$-$Ln^{III}(NO_3)_3]$ {Ln = Dy (**2**), Tb (**4**), Ho (**6**), and Er (**8**)} (here H_2L = *N*,*N*′-bis (3-methoxysalicylidene)-1,3-diamino-2,2-dimethylpropane) (see Scheme 1 for generic representation of these structures).[21b] By performing this study, we desire to resolve the following interesting queries: (i) How accurate are the Lines model of extracting exchange coupling in {3d-4f} complexes? (ii) How the single-ion anisotropy varies across complexes **1**−**8**? Given the fact that complexes **1**−**4** and **5**−**8** are structurally analogous, this provides a rare chance to evaluate the evolution of single-ion anisotropy with an increase in the 4f occupation. (iii) What is the mechanism of magnetic coupling in this anisotropic {3d-4f} pair? As the *J* values ranges from +2.3 to −0.2 cm^{-1} for complexes **1**−**8**, this is an ideal test set to affirm the mechanism of magnetic coupling. (v) How magnetic exchange interactions influence the magnetization relaxation in these complexes? (vi) Can the exchange be fine-tuned so as to increase the effective barrier?

2. COMPUTATIONAL DETAILS

All the post-Hartree−Fock ab initio calculations were enumerated using the MOLCAS 7.8 suite.[26] Notable aptness of CASSCF/RASSI-SO/SINGLE_ANISO[26c,27] methodology toward the illustration of magnetic characteristics of lanthanide complexes[24b−e,28] has driven us to perform our study via this approach.

The Lines model[18a,19d,29] has been used to depict the exchange interaction between the true spins of the metallic sites using the above acquired lowest spin−orbit states (see details in Supporting Information computational details). The Lines[29b] model has been proven to be beneficial owing to its intrinsic single parameter (*J*)

DOI: 10.1021/acs.inorgchem.6b01831
Inorg. Chem. 2016, 55, 11201−11215

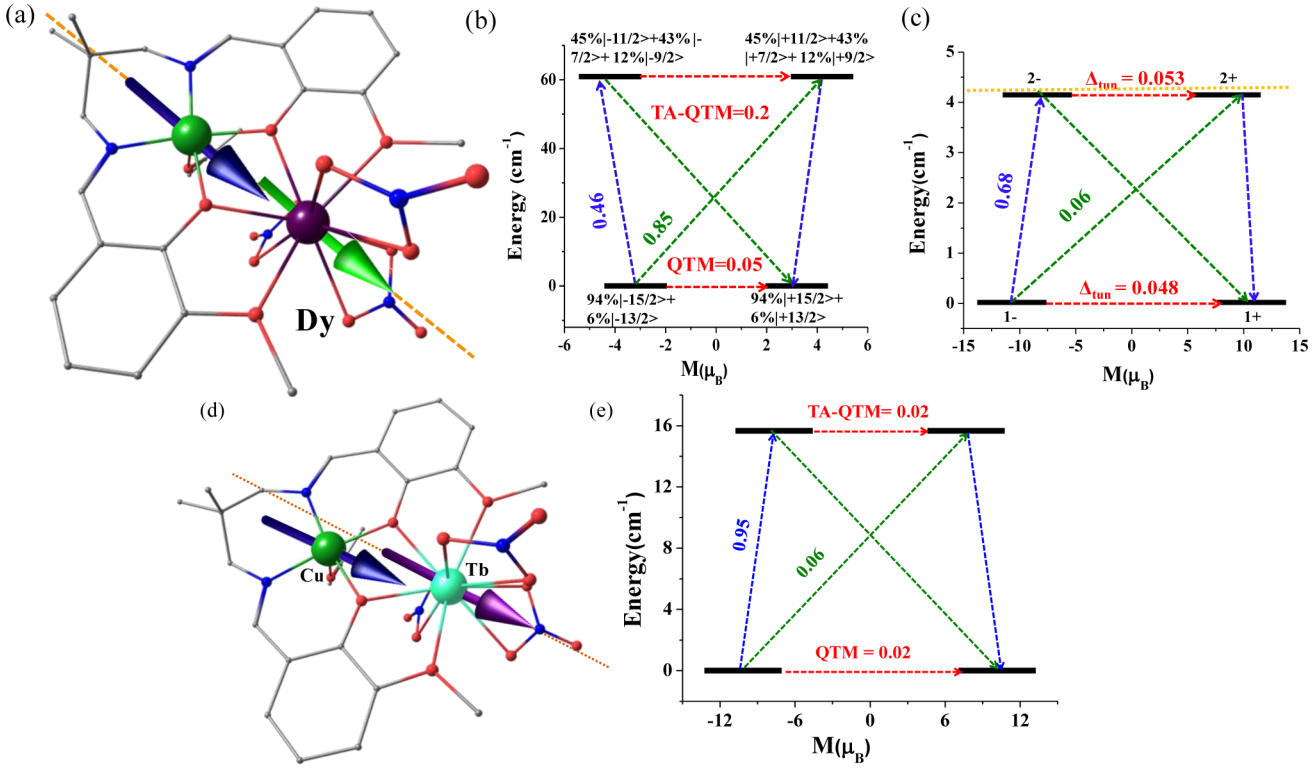

Figure 1. (a) Molecular structure of **1**, where H atoms were removed for clarity, the light green arrow on Dy^{III} and blue arrow on Cu^{II} correspond to the orientation of the local magnetic moment in the ground exchange doublet state, respectively, while the orange line implies the main magnetic anisotropy axis of the Dy^{III} ion{color code: Dy: purple, Cu: green, O: red, N: blue, C: gray}. (b) Ab initio SINGLE_ANISO[45] computed magnetization blocking barrier for **1**. (c) Ab initio POLY_ANISO[44] computed low-lying exchange spectrum and magnetization blockade barrier (4.15 cm^{-1}; yellow dashed line) for **1**. The *x*-axis indicates the magnetic moment of each state along the main magnetic axis of complex **1**, while the *y*-axis denotes the energy of the respective states. The thick black lines imply the Kramers doublet as a function of magnetic moment. All the dotted (red/green/blue) lines imply averaged matrix element of the transverse magnetic moment connecting corresponding states, i.e., $(|\mu_x| + \mu_y| + \mu_z|)$ /3. The dotted blue/green lines indicate the most probable relaxation process (Orbach process composed of direct/Raman pathway) following the minimum energy path where transition matrix elements connecting the states with reverse magnetization is largest. The dotted red lines correspond to the QTM/TA-QTM of relaxation contribution between the connecting pairs. The numbers provided at each arrow are the mean value for the corresponding matrix element of the magnetic moment. The black texts near the black lines reveal the nature of the Kramers Doublets in terms of major wave function contribution. (d) Molecular structure of **3**, where H atoms were removed for clarity {color code: Tb: light green, Cu: dark green, O: red, N: blue, C: gray}. (e) Ab initio POLY_ANISO[44] computed low-lying exchange spectrum and position of the magnetization blocking barrier (15.67 cm^{-1}; yellow dashed line) for **3**.

consideration (approximating isotropic exchange interaction in the absence of spin−orbit coupling on metal centers) for interacting metal pair. The Lines exchange parameters can be procured from the least-squares fitting of the magnetic properties based on ab initio computed lowest spin−orbit energy multiplets on the magnetic centers. From the exchange eigenstates, magnetic properties of dinuclear complexes as well as parameters of pseudospin Hamiltonian can be derived. The Lines exchange coupling followed by the estimation of the magnetic properties of the dinuclear complex were undertaken using the POLY_ANISO[44] program, interfaced with the SINGLE_ANISO[45] module treating metallic fragments individually. The resultant exchange spectrum and correlated wave functions of the dinuclear complexes were used to determine magnetic properties of the dinuclear complexes. For all the eight complexes studied, only one exchange interaction $J_{Cu/VLn}$ has been employed as a fitting parameter. Additionally, the intermolecular interaction (z*J*) has been considered within the mean field approximation. To obtain an estimate of the magnetic anisotropic exchange between Ln^{III} and Cu^{II}/V^{IV}, we fitted the magnetic susceptibility data using the Lines model {which uses the Ising Heisenberg exchange Hamiltonian, $\hat{H} = -J\hat{s}_{Lnz}\hat{s}_{Cuz/Vz}$; ($\hat{s}_{Lnz}\hat{s}_{Cuz/Vz}$ represent projections of the effective spin $\tilde{s} = 1/2$ of lowest energy multiplet of Ln^{III} ions and Cu^{II}/V^{IV} ions) to treat both anisotropic dipolar and exchange interactions} as embedded in the POLY_ANISO[44] routine including the dipolar exchange (see Supporting Information for further details). Notably, this program uses SINGLE_ANISO computed energies, and the wave function of the corresponding Ln^{III} ions (Cu^{II}/V^{IV} have been considered to be isotropic with the constant *g* values of 2.25 and 1.96 respectively).

Besides using the Lines approach to compute the *J* values, we have also employed the ORCA 3.0[30] suite of programme (DFT and broken symmetry (BS)[31] approach) to compute the exchange (J_{MLn}) values to further validate the interactions deduced. To estimate the *J* values using DFT, {Cu−Gd} or {V−Gd} models are employed. These calculations are performed using the B3LYP functional and SARC-DKH[32] basis set as this approach has been extensively employed to extract exchange coupling in {3d-Gd}[33] complexes. Later, the obtained *J* values have been rescaled to the pseudospin 1/2 of the corresponding lanthanide atoms.[3d]

3. RESULTS AND DISCUSSION

In all the eight complexes studied, the lanthanide^{III} ion is 10 coordinated with six nitrate oxygen atoms, two methoxy oxygen atoms, and two bridging phenolate oxygen atoms (see Figure 1). The Cu^{II} ion possesses a square pyramidal coordination composed of imine nitrogen atoms and phenolate oxygen atoms at the equatorial sites and an acetone molecule at the axial site. The V^{IV} ion on the other hand shows a compressed

DOI: 10.1021/acs.inorgchem.6b01831
Inorg. Chem. 2016, 55, 11201−11215

Table 1. Computed Anisotropic *g*-Tensor Values (g_{xx}, g_{yy}, and g_{zz}) Obtained from Single-Ion Anisotropy Calculation As Well As for Exchange Coupled States, Exchange Interaction Estimated Using Experiments and Lines Model (cm^{-1}), Computed U_{cal} and Experimental U_{eff} Values (cm^{-1}), Computed Tunnel Splitting (cm^{-1}) between the Exchange Coupled States for Complexes 1−8

	SINGLE_ANISO[45] estimates			POLY_ANISO[44] estimates								
complexes	g_{xx}	g_{yy}	g_{zz}	g_{xx}	g_{yy}	g_{zz}	Δ_{tun}:GS	J (Lines)	U_{cal}	J (exp)	U_{eff}[a]	SMM behavior
1	0.01	0.28	19.12	0	0	21.39	0.048	1.55	4.15	1.13	7.99	yes
2	0.31	0.93	17.57	0	0	19.20	0.008	0.15	0.45	0.19		no
3	0	0	17.84	0.08	0.08	20.31	4.2×10^{-7}	5.30	15.67	>2.3	29.40	yes
4	0	0	17.44	1.58	1.96	2.59	1.9×10^{-9}	0.06		0.04		no
5	0	0	16.43	2.07	2.26	8.66	8.5×10^{-9}	1.05		0.76		no
6	0	0	17.04	2.23	1.61	0.53	4.3×10^{-8}	−0.18		−0.13		no
7	3.45	5.17	10.34	0	0	12.39	0.01	0.24	0.36	0.17		no
8	0.98	1.03	14.66	0	0	16.55	5.6×10^{-4}	−0.02	0.27	−0.01		no

[a]It is worthy to mention that the experimental U_{eff} values have been extracted using a dc bias field of 1000 Oe and the two complexes (**1** and **3**) show field-induced (1000 Oe) SMM behavior.

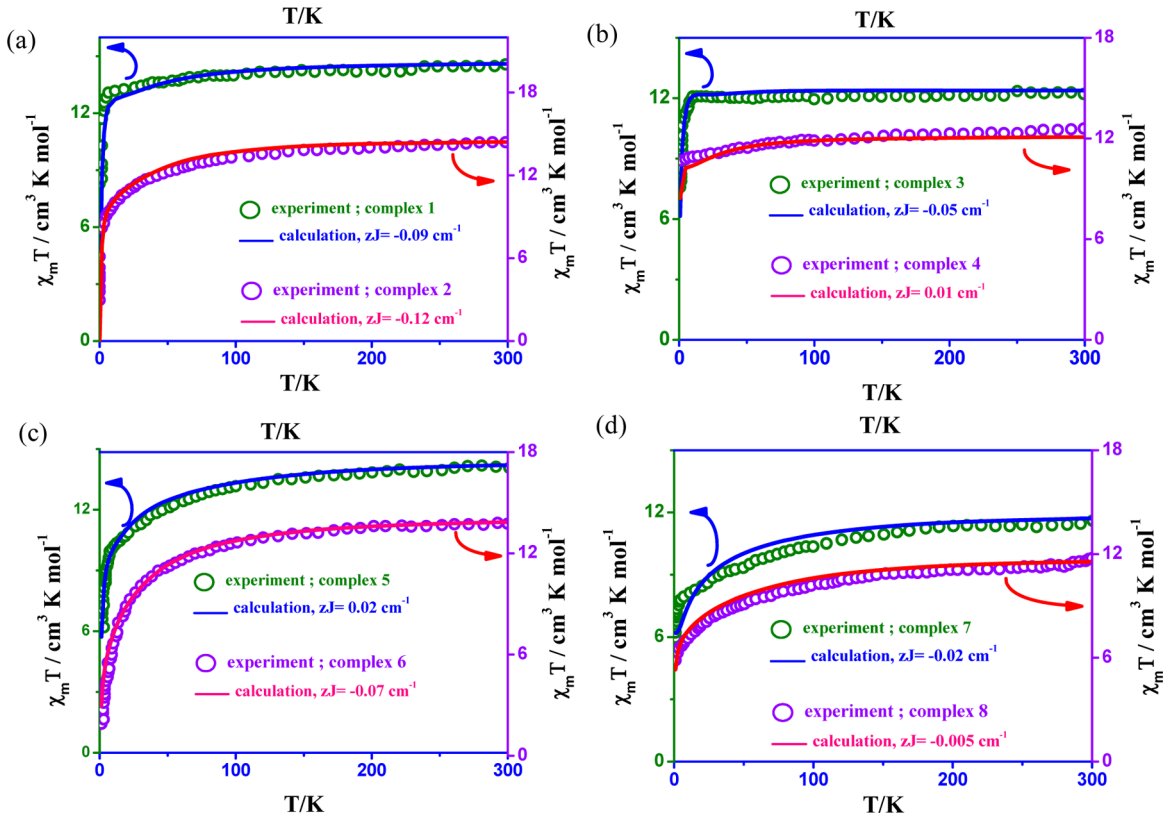

Figure 2. Variable temperature magnetic susceptibility (χT) data for (a) complexes **1** and **2**, (b) complexes **3** and **4**, (c) complexes **5** and **6**, (d) complexes **7** and **8** where the respective void circles represent experimental data, while the solid line imply fit employing the Lines model. The data have been plotted using a double-*y* plot where individual *y*-axis of the complexes is noted by the arrows. For complexes **1** and **2** the experimental data has been scaled by a factor 1.08,[35] while for rest of the complexes the data have been used as such.

octahedron with imine nitrogen atoms and phenolate oxygen atoms at the equatorial sites, an acetone molecule and a short oxo cap at the axial site (see Figures 1a,d and 3). The detailed analysis of the individual molecules is presented first where we begin our discussion with single-ion anisotropy of individual Ln^{III} ions. This is followed by the discussion on the exchange-coupled states. Later the magnetic properties and the exchange interactions among complexes **1**−**8** are discussed in detail along with some magneto-structural correlations.

Studies on $[Cu^{II}(L)(C_3H_6O)Dy^{III}(NO_3)_3]$ Complex (1). We have evaluated eight low lying Kramers doublets (KDs) for the Dy^{III} ion corresponding to the $^6H_{15/2}$ state. These states spread over the energy window of 443.7 cm^{-1} with $m_J = \pm 15/2$ being the ground state. Ground state of the Dy^{III} ion in **1** (g_{xx} = 0.01, g_{yy} = 0.28, and g_{zz} = 19.12, see Table 1, Table S2, and Figure 1a for orientation of ground state g_{zz} tensor) is axial in nature with concomitant transverse components leading to non-negligible QTM effects (transversal magnetic moment corresponding to QTM relaxation pathway = 0.05 μ_B, see Figure 1b) within the ground state Kramers doublets (KDs). The large value of g_{zz} reveals the presence of a large magnetic moment, proceeding toward the expected g_{zz} = 20 pertinent to $m_J = \pm 15/2$ state (see Figure 1a). This is in agreement with HF-EPR measurement.[21b] Our calculations postulate a dominant single-ion relaxation to be channelled via the first excited state leading to the estimation

DOI: 10.1021/acs.inorgchem.6b01831
Inorg. Chem. 2016, 55, 11201−11215

of 60.9 cm^{-1} as the calculated energy barrier (U_{cal}, see Figure 1b).

Experimentally complex **1** is characterized as a field induced SMM possessing effective energy barrier (U_{eff}) of 7.99 cm^{-1}. However, the calculated barrier U_{cal} is significantly higher than the experimental U_{eff} barrier, and this reveals that the mechanism of relaxation is unlikely to be single-ion in origin. This is affirmed by the fact that structurally analogous $\{Zn^{II}Dy^{III}\}$ complexes ($[Zn(\mu\text{-}L)(\mu\text{-}OAc)Dy(NO_3)_2]$, $[Zn(\mu\text{-}L)(\mu\text{-}9\text{-}An)Ln(NO_3)_2]$\{$H_2L$ = *N*,*N*′,*N*″-trimethyl-*N*,*N*″-bis (2-hydroxy-3-methoxy-5-methylbenzyl) diethylenetriamine }; $[Dy_2Zn_2L_2(BA)_6]$ {L = 1,2-bis(2-hydroxy-3-methoxybenzylidene)hydrazine; BA = benzoic acid)}; $[ZnDy(NO_3)_2(L)_2(CH_3CO_2)]$ {HL = 2-methoxy-6-[(*E*)-phenyliminomethyl]phenol) exhibit larger U_{eff} values.[19b,24b,20,34] The ground state QTM can be best illustrated by the crystal field parameters subject to the negligible contributions from intermolecular and hyperfine interactions. The corresponding crystal field Hamiltonian can be expressed as

$$\hat{H}_{CF} = \sum_{k=-q}^{q} \sum^{q} B_k^q \tilde{O}_k^q$$

where B_k^q implies crystal field parameter and O_k^q represents Stevens operator. Larger (see Table S18) non-axial B_k^q (where $q \neq 0$, K = 2, 4, 6) terms compared to their corresponding axial B_k^q (where q = 0, K = 2, 4, 6) terms are found to favor QTM process. Here, however, both the axial and the non-axial terms are found to be equal in strength postulating non-negligible relaxation via the ground state KD (see Table S18 in Supporting Information) as per earlier establishments.[42,43,49]

Ab initio calculations postulate that slow relaxation observed for this complex is dictated mainly by the exchange coupled multiplets incurred by Cu---Dy interactions. The anisotropic exchange coupling parameter J is the summation of exchange interaction (J_{exch}) and magnetic dipole−dipole coupling ($J_{dipolar}$). SINGLE_ANISO derived ground state g-matrix enables precise computation of $J_{dipolar}$ and unknown J_{exch} can be estimated by fitting magnetic data. The isotropic *g*-tensor of Cu^{II} is estimated to be 2.25 (see Table S3 in Supporting Information), and this has been utilized in the POLY_ANISO[44] program (see Figure 2a, top). This enables us to estimate the exchange interaction J_{CuDy} as +1.55 cm^{-1} ($\hat{H} = -J\hat{S}_{Dy}\hat{S}_{Cu}$) for complex **1** (see Tables S41 and S42 for standard deviation and mean absolute error). To further validate our computed exchange parameter, we have also computed the exchange parameter through BS-DFT calculations (see Table S19). This calculation[3d] yields +1.05 cm^{-1} as the exchange interaction, and this is closer to the estimate obtained using POLY_ANISO[44] as well as HF-EPR study (see Figure 1c). The net exchange interactions have two contributions: exchange and dipolar, and it is an established fact that the DFT calculations yield only the exchange part of the J, while the J values obtained from the fit contains both contributions (see Supporting Information, Table S40). This estimates the dipolar contributions as +1.14 cm^{-1} for complex **1**. Besides we have also attempted to fit only the low temperature data (2−50 K) using Lines model, and these data also yield very similar J values (see Figure S9 in Supporting Information and Table S40 in Supporting Information). As the experimental J value is well evaluated (HF-EPR and magnetic data), this offers a rare chance to validate the computed values with respect to the experimental data. A very good match between the two values (cal vs exp as +1.55 cm^{-1} vs +1.13 cm^{-1}; see Tables S41 and S42 for standard deviation and mean absolute error) postulates that the employed methodology is accurate and can be employed to extract such intricate parameter for {3d-4f} molecular magnets.

For complex **1**, six exchange Ising doublets have been obtained from six lowest lying KDs on the Dy^{III} site and two components of the Cu^{II} site giving rise to (6*2) = 12 energy levels (see Table S5). The exchange states in Figure 1c are arranged in compliance with their corresponding maximal magnetic moments. The lowest exchange levels have been grouped into doublets, and these doublets are split by tunnel splitting indicated in Figure 1c as Δ_{tun} (due to Kramers nature of the exchange coupled system). For all the exchange-coupled states, the transverse components are found to be nearly zero ($g_{xx} = g_{yy} = 0 < 1 \times 10^{-9}$), and orientation of the magnetic anisotropy of the ground state resembles that of Dy^{III} single-ion behavior. Besides, the local magnetic moment of Cu^{II} ion is also found to lie along the main magnetic axis. The magnetic relaxation in the exchange-coupled states is estimated by the tunnel splitting parameter Δ_{tun}, and for the ground state this is estimated to be 10^{-2} cm^{-1}, indicating efficient QTM between the ground state. This suggests the absence of any SMM behavior at zero-field for complex **1**, and in fact an application of 1000 Oe dc field is required to observe the relaxation. This strongly supports the computed relaxation mechanism depicted in Figure 1c.

The first excited exchange doublet lies at 4.15 cm^{-1} higher in energy from the ground state and our calculations predict that there is a significant Raman/Orbach process (see Figure 1c) via the first excited state. Besides, the first excited state also possesses large Δ_{tun}, suggesting a favorable TA-QTM process. Application of 1000 Oe dc field is expected to quench the QTM between the ground states to a certain extent, leading to the observation of magnetic relaxation. In the applied field scenario, the major relaxation is expected to channel via the first excited state, leaving the estimate of U_{cal} as 4.15 cm^{-1}, and this is close to the experimental estimate.

Studies on $[V^{IV}O(L)(C_3H_6O)Dy^{III}(NO_3)_3]$ Complex (2). For complex **2** the energy span of the low lying eight KDs is found to be 356.3 cm^{-1}. The ground state anisotropy (g_{xx} = 0.31, g_{yy} = 0.93, and g_{zz} = 17.57, see Table S6, S18 and Table 1) shows axiality with concomitant transverse anisotropy. This suggests the ground state to be $m_J = \pm 15/2$ (with small contribution from higher energy excited state) state and is in accord with the HF-EPR data ($g \approx 13-18$). Besides for this complex, the signals at $g \approx 18$ are obtained at lower temperature, and this strikingly matches with our estimated g_{zz} value.[21b] In this complex, the transverse magnetic anisotropy has been more prominent as compared to complex **1** leading to a prominent QTM effect (0.21 μ_B, see Figure S1a). This suggests the absence of any SMM behavior in complex **2** corroborating experimental observations. Utilizing $g \approx 1.98$ for V^{IV} (see Table S7 in Supporting Information), POLY_ANISO[44] program yields J_{VDy} exchange interaction as +0.15 cm^{-1} (J_{exp} + 0.19 cm^{-1} ; see Figure 2a bottom; see Tables S41 and S42 for standard deviation and mean absolute error). The Δ_{tun} within the ground exchange doublets found to lie in the order of 10^{-3} cm^{-1}, indicating sufficient QTM to be operative (Figure 4a and Table S9). Still, the anisotropic nature of the ground exchange doublets will push the relaxation further upward to the next excited state lying at an energy separation of 0.45 cm^{-1} with respect to the ground exchange doublet. Now, the

DOI: 10.1021/acs.inorgchem.6b01831
Inorg. Chem. 2016, 55, 11201−11215

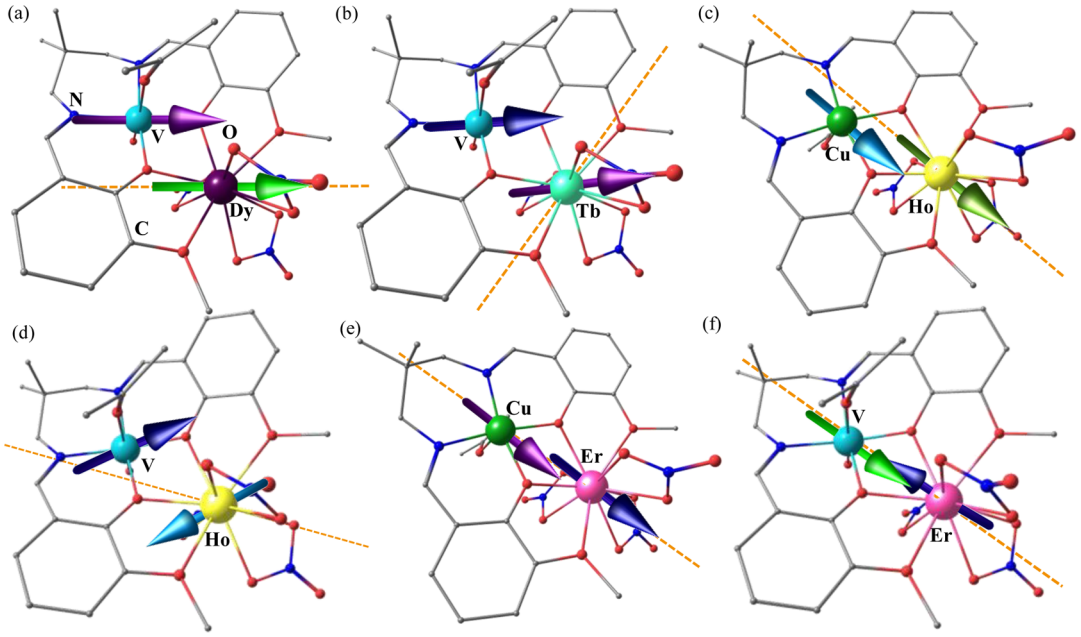

Figure 3. Molecular structures of complexes (a) **2**, (b) **4**, (c) **5**, (d) **6**, (e) **7**, and (f) **8**. The H atoms have been removed for clarity, the solid filled arrows on Dy^{III}{**2**}, Tb^{III} {**4**}, Ho^{III}{**5**/**6**}, Er^{III}{**7**/**8**}, Cu^{II}{**2**,**4**,**5**−**8**}, and V^{IV} {**2**,**4**,**5**−**8**} corresponds to the orientation of the local magnetic moment of the respective Ln^{III} and Cu^{II}/V^{IV} ions in the ground exchange doublet state respectively, while the dashed line in all the figures implies the main magnetic anisotropy axis of the respective complexes {color code: Tb: light green, Cu: dark green,V: sky bue, Ho: yellow, Er: pink, O: red, N: blue, C: gray}.

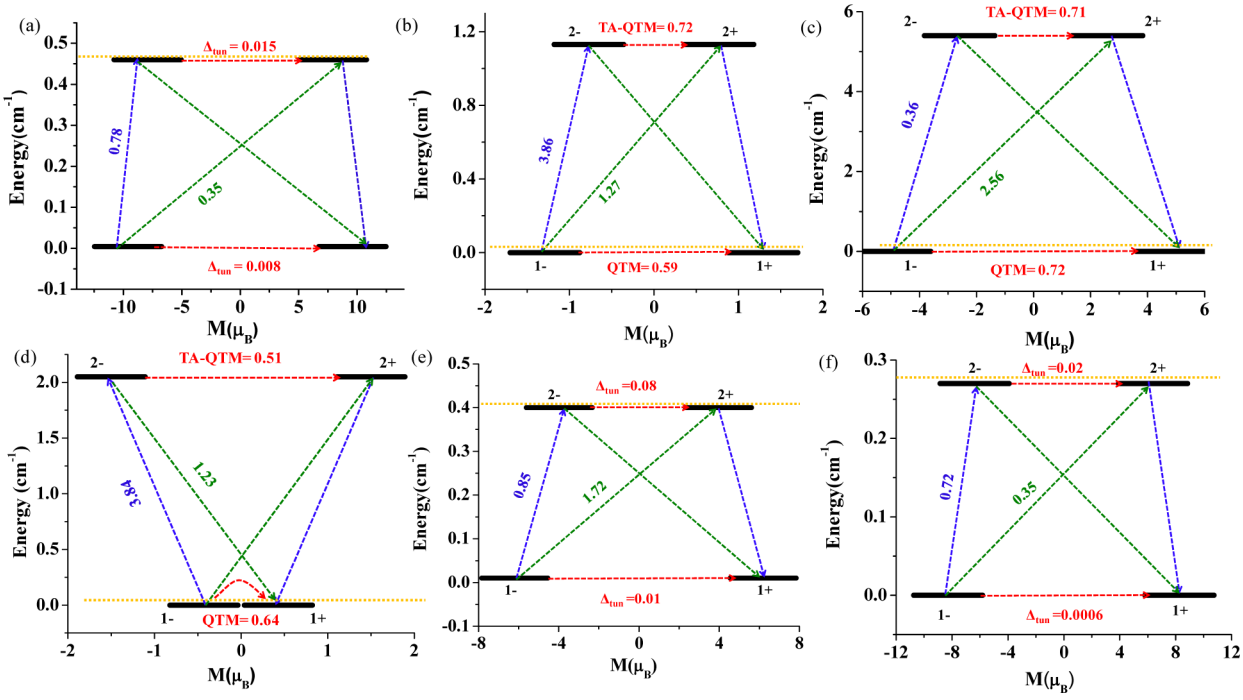

Figure 4. Ab initio POLY_ANISO[44] computed low-lying exchange spectrum and position of the magnetization blocking barrier (denoted by yellow dashed line in all the figures) in complex (a) **2**, (b) **4**, (c) **5**, (d) **6**, (e) **7**, and (f) **8** (see Figure 1 caption for detailed description).

observed tunnel splitting ($0.015 > 10^{-5}$ order) between the ±2 states is significant, and this enforces relaxation via this state, placing the U_{cal} estimate as 0.45 cm^{-1}. Besides, the very weak exchange interaction between V^{IV}−Dy^{III} ions leads to the independent orientation of magnetic moment for the V^{IV} ions at lower temperatures, and this offers a fluctuating magnetic field for the Dy^{III} ion leading to a very fast relaxation as observed in the experiments.[35b] The local magnetic moment of V^{IV}, Dy^{III} and the main magnetic axis of the DyV molecule are found to be collinear (see Figure 3a). We would like to note here that for both the complexes (**1** and **2**), the ab initio computed anisotropy axis is found to lie closer to the electrostatic anisotropy axis.[8h,13b,c]

Studies on $[Cu^{II}(L)(C_3H_6O)Tb^{III}(NO_3)_3]$ Complex (3). We have computed 13 energy levels (five pseudo-doublets and three singlets) corresponding to J = 6 for the Tb^{III} ion in

DOI: 10.1021/acs.inorgchem.6b01831
Inorg. Chem. 2016, 55, 11201−11215

complex **3**. The ground state is estimated to be $m_J = \pm 6$ state (g_{zz} = 17.84); however, large tunnel splitting (0.31 cm^{-1} see Figure 4a, Table 1 and S10) deters SMM characteristics with major relaxation via this state. It is notable that such a large Ising (large g_{zz}) type ground state indicates the presence of Ising type exchange interaction between the two neighboring centers in complex **3**. The Lines model yields J_{CuTb} as +5.3 cm^{-1} (see Figure 1d and Figure 2b, top; see Tables S41 and S42 for standard deviation and mean absolute error), and this complies well with the experimental estimate (noted as J_{CuTb} > 2.3 cm^{-1}). This postulates rather a strong ferromagnetic interaction between the Cu^{II} and the Tb^{III} ion and is in line with the other J_{CuTb} exchange reported.[52] Unlike in single-ion, the exchange coupled ground state (see Figure 1e) is found to possess non-negligible transverse components (see Table S13, g_{xx} = 0.06 and g_{yy} = 0.06) due to the overall Kramers nature of the exchange-coupled system. A similar scenario has been detected also for the first excited state (g_{xx}= 0.02 and g_{yy} = 0.08). This was further substantiated by significant transversal moment matrix elements pertinent to the QTM/TA-QTM (0.02/0.02 μ_B) contribution to the magnetic relaxation mechanism (see Figure 1e).

However, considerable off-diagonal transition moment matrix elements between the −1 and +2 and −2 and +1 (0.09 μ_B ; green arrow in Figure 1e) have been observed. Apart from these, significant average matrix elements (red dotted arrows in Figure 1e) of the magnetic moment connecting ±1 and ±2 (0.91 μ_B) states is also detected (corresponds to the most probable relaxation pathway). Hence, despite the large predominant g_{zz} components, the magnetic relaxation is likely to take place via the first excited state, and this places the U_{cal} value as 15.7 cm^{-1}. The experimental estimate of U_{eff} is 29.4 cm^{-1}, and this is higher than the theoretical estimate. However, as the barrier height is estimated in the presence of an applied field which is known to quench the relaxation pathways, larger than the theoretical estimate is rather expected.

Studies on $[V^{IV}O(L)(C_3H_6O)Tb^{III}(NO_3)_3]$ Complex (4). Here the 13 spin−orbit states of J = 6 are found to spread over 272.8 cm^{-1} for Tb^{III} ion. Here also, the anisotropies are of pure Ising type with g_{zz} = 17.44 (Figure 5b, dashed line and evident from the experimental HF-EPPR study of $g \approx 15$) for the ground state pseudo-doublet. The tunnel splitting within the ground pseudo-doublet is extremely large (1.13 cm^{-1}, see Table S14), much higher than that found on complex **3**. This suggests significant QTM within the ground state and precludes any SMM characteristics for complex **4**. The POLY_ANISO[44] program yields J_{VTb} exchange as +0.06 cm^{-1} (J_{exp} + 0.04 cm^{-1}; see Table 1, Figure 2b, bottom and Tables S15 and S17 in Supporting Information and Figure 3b; see Table S41 and S42 for standard deviation and mean absolute error). The ground state g-tensors of exchange coupled states are estimated to be nearly isotropic in nature (g_{xx} = 1.8,g_{yy} = 1.96, g_{zz} = 2.59, see Table S17) as exemplified by substantial transversal moment matrix elements pertinent to the QTM/TA-QTM process (0.59/0.72 μ_B) (see Figure 4b). This suggests that complex **4** is unlikely to possess any SMM behavior and is in line with the experimental observation. As the exchange interaction is extremely weak, it has no role on the magnetization blockade. Besides, it is worthy to mention here that, although the local magnetic moments of Tb^{III} and V^{IV} align parallel to each other (see Figure 3b), the orientation of the exchange-coupled state is tilted compared to the single-ion behavior.

Studies on $[M(L)(C_3H_6O)Ho^{III}(NO_3)_3]$ (M = Cu^{II}, V^{IV} Complexes (5 and 6). The 17 spin orbit-coupled states of Ho^{III} corresponding to J = 8 state are found to lie within ∼385 cm^{-1} energy for both complexes **5** and **6** (see Tables 1 and S21 and the principal magnetic anisotropy orientation). A large ground state tunnel splitting (4.8 and 2.4 cm^{-1} for **5** and **6** respectively) has been detected in the ground state, and this precludes the observation of magnetic bistability for both complexes **5** and **6** (Figure 4c,d). The POLY_ANISO[44] program yields J_{CuHo} as +1.05 cm^{-1} for complex **5** (J_{exp} + 0.76 cm^{-1}; see Figure 2c, top). Similarly for complex **6**, J_{VHo} is estimated as −0.18 cm^{-1} (J_{exp} −0.13 cm^{-1} ; see Figure 2c, bottom; see Tables S41 and S42 for standard deviation and mean absolute error), and here the interaction is found to be antiferromagnetic in nature unlike in other cases. Also for the exchange coupled state, a large transverse component (g_{xx} = 2.07, g_{yy} = 2.26, g_{zz} = 8.66 for complex **5** and g_{xx} = 2.23, g_{yy} = 1.61, g_{zz} = 0.53 for complex **6**, see Figure 3c,d for computed orientations and Table S21 and S25) has been detected which is expected to facilitate a very fast QTM (0.72 and 0.64 μ_B for **5** and **6** respectively; see Figure 4c,d) process within the ground state for both **5** and **6**. For complex **5**, although J value is moderate, the g-anisotropy of both the single-ion and the exchange-coupled states (see Table S24 for complex **5** and S28 for complex **6**) are unfavorable leading to the absence of SMM behavior, and this is affirmed by the experimental studies.

Studies on $[M(L)(C_3H_6O)Er^{III}(NO_3)_3]$ (M = Cu^{II} and V^{IV} Complexes (7 and 8). The single ion anisotropy study on Er^{III} leads to eight Kramers doublets {$^4I_{15/2}$ for Er^{III}, Kramers ion} pertaining to J = 15/2 states. They are found to lie in an energy span of 416 and 407 cm^{-1} for complexes **7** and **8** respectively (see Table 1, Tables S29 and S33). Large transverse anisotropy {g_{xx} = 3.45, g_{yy} = 5.17, g_{zz} = 10.34 (reflected in experimental HF-EPR study as $g \approx 13$) and g_{xx} = 0.98, g_{yy} = 1.03, g_{zz} = 14.66 (reflected in experimental HF-EPR study as $g \approx 9-13$) for complexes **7** and **8** respectively} of the ground state KD (see Figure 3e,f and Table 1, S29 and S33) reveals a non-axial nature of the ground state. This is evidenced by our quantitative magnetic relaxation mechanism with QTM of 1.43 μ_B and 0.33 μ_B for complexes **7** and **8** respectively (see Figure S1b,c) based on single-ion analysis. This is much larger than that observed for complexes **1** or **2** and suggests QTM in the ground state as a major relaxation pathway. POLY_-

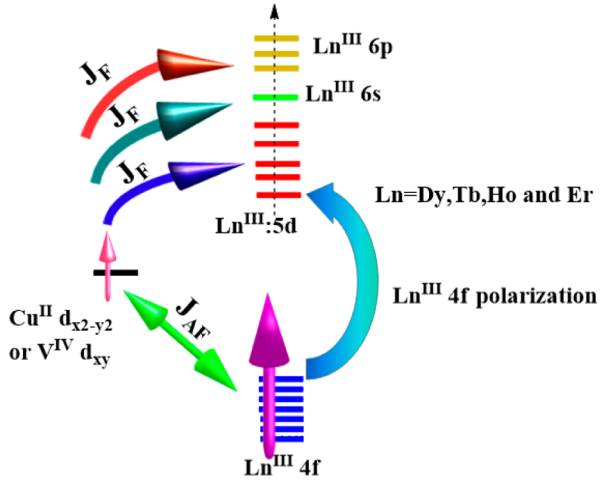

Figure 5. Schematic representation of the plausible magnetic exchange coupling mechanism operative in all the eight studied complexes.

DOI: 10.1021/acs.inorgchem.6b01831
Inorg. Chem. 2016, 55, 11201−11215

ANISO[44] program yields J_{CuEr} as +0.24 cm^{-1} (J_{exp} + 0.17 cm^{-1}), while the J_{VEr} interaction is estimated as −0.02 cm^{-1} (J_{exp} −0.01 cm^{-1}) (see Figure 2d and see Tables S41 and S42 for standard deviation and mean absolute error). For complex **7**, significant Δ_{tun} has been detected (0.01, see Figure 4e) within the ground exchange doublets instigating the relaxation via this level. Contrary to this, strong axiality of the ground exchange doublet (g_{xx} = 0, g_{yy} = 0 and g_{zz} = 12.39, see Table S32) tries to push magnetic relaxation upward via the excited exchange doublet; however, a weak exchange interaction places the first excited exchange coupled state at merely 0.4 cm^{-1} (see Figure 4e) higher in energy rationalizing the absence of SMM behavior in this complex. For complex **8** on the other hand, the ground exchange doublet is associated with smaller tunnel splitting (~10^{-4} cm^{-1}) and huge axiality (g_{zz} = 12.39 ≫ g_{xx} = g_{yy} = 0). This enforces the magnetization to move upward to the first excited state. However, the first excited state is found to lie at 0.27 cm^{-1} (see Figure 4f) higher in energy leading to again the absence of any SMM characteristics also for complex **8** (see Figure 4f and Table S36).

4. DISCUSSION AND COMPARATIVE STUDY OF COMPLEXES 1−8

Single-Ion Anisotropy. The lanthanide environment in all eight complexes reported is analogous, yet only complexes **1** and **3** exhibit field induced SMM behavior. All the lanthanide ions have 10 coordination, and SHAPE[41,] analysis using continuous shape measures (CShMs) reveals that the distortion parameter for all the lanthanide ions are in the range of 2.4−2.8 compared to the ideal "sphenocorona" structure (C_{2v} point group). Although the deviation found among the structures is marginal, it has a significant influence on the single-ion anisotropy. The {Ln-Cu} complexes with Cu^{II} ion are found to be less distorted compared to their V^{IV} {Ln-V} analogues (2.5 vs 2.7 for complexes **1** and **2** respectively; 2.6 vs 2.8 for complexes **3** and **4** respectively). All aforementioned divergences imply the extent of deviation from idealized 10-coordinated sphenocorona geometry considering the ligand field surrounding lanthanide. The less distorted structures are found to have larger barrier heights, less QTM/tunnel splitting, etc., suggesting that even minor deviations in structures are important in deciphering the magnetization relaxation.

The Dy^{III} ion in complexes **1** and **2** possesses oblate electron density[12] where weak equatorial ligation and strong axial ligation enhance the barrier height. Both in complexes **1** and **2**, the bridging μ-phenoxo oxygen atoms and a nitrate group serve in the axial position, while in the equatorial position, two methoxy oxygen atoms and two nitrates are coordinated. This is affirmed in the CASSCF results where the axial anisotropy lies along the Dy^{III}−Cu^{II} bond vector.

The proximity to the +2 charge Cu^{II} cation leads to a significant negative charge on the bridging oxygen atoms leading to a stronger axial interaction (reflected in the computed CASSCF charges). However, on the radial plane of the Dy^{III} ion, two nitrate groups are present along with two methoxy oxygen atoms which offer less electrostatic repulsion. Thus, the ligand environment is ideally suited for an oblate Dy^{III} ion leading to the stabilization of the m_J = ± 15/2 ground state. For complex **2** on the other hand, the V^{IV}═O bond distorts the ligand environment and the planarity of the molecule (see Figure S7 in Supporting Information for superimposed structures of **1** and **2**). This leads to a deviation in the direction of the g_{zz} axis by about ~40 deg from the Dy^{III}−V^{IV} bond vector. Besides, the ground state is not a pure m_J = ± 15/2 state as it is strongly mixed with the m_J = ± 13/2 state (see Figure S1 in Supporting Information). This significant difference observed in the magnetic anisotropy between **1** and **2** is essentially due to the structural differences which are influenced primarily by transition metal ions.

As the ligand field is well suited to the oblate ion, the non-Kramers Tb^{III} ion is also expected to exhibit SMM behavior (as in complex **3**). Here as well, the less distorted Tb−Cu complex possesses less tunnel splitting (0.31 cm^{-1}) and SMM behavior, while the strongly distorted (strongest among all) Tb−V complex (**4**) possesses larger tunnel splitting (1.13 cm^{-1}) leading to the absence of SMM behavior. The g_{zz} direction computed for complex **3** resembles that of **1**; i.e., it lies nearly along the Tb^{III}−Cu^{II} bond vector, while for complex **4**, it resembles that of complex **2** (deviation is ~85°). A similar trend is visible also for Ho^{III} complexes **5** and **6**. However, here, both the complexes do not exhibit SMM behavior as they possess very large tunnel splitting. For the prolate Er^{III} ions on the other hand, the ligand field set up is not best suited and stronger axial ligation, and an asymmetric nature of the coordination environment leads to strong mixing of the m_J levels. This leads to a significant QTM process. This is particularly evident in complex **7** where the ground state is determined to be 47%| ± 13/2>+40% | ± 7/2> demonstrating the extent of the m_J level mixing at the ground state.

Mechanism of Magnetic Coupling. The magnetic exchange between this pair is of paramount importance as at several instances stronger exchange interactions are found to oppress the QTM behavior leading to enhanced SMM properties.[3d,14,18a,19d,f,g,25b,36] To understand the origin of magnetic coupling, the mechanism of magnetic coupling for a 3d-4f ion needs to be analyzed.

Qualitative mechanism of magnetic coupling has been proposed for a {3d-4f} pair by Kahn and Gatteschi stressing the importance of 5d and 6s orbitals respectively in the magnetic coupling.[47] A general schematic mechanism adapted for 3d-4f complexes based on earlier[33,37] CASSCF and DFT calculations is shown in Figure 5. In order to gain further understanding on the mechanism of exchange interaction, we have performed molecular orbitals (MO) and natural bond orbitals (NBO) analysis for all the complexes based on the BS-DFT merhod.[33]

The Cu^{II} ion possesses the unpaired electron in the $d_{x^2-y^2}$ orbital, while the V^{IV} ion has the unpaired electron in the d_{xy} orbital. Although the V^{IV} ion can possess orbital contribution to the magnetic moment, the distorted nature of the coordination around V^{IV} leads to splitting of the t_{2g} orbitals with the d_{xz}/d_{yz} orbitals found to lie ~6700 cm^{-1} higher in energy, rendering an isotropic picture similar to that of the Cu^{II} ion. Thus, these two metal ions are expected to influence the J values differently. The antiferromagnetic part of J (J_{AF}) arises from the overlap between the magnetic orbitals of the 4f ion and the 3d orbitals, while the ferromagnetic contributions to the net J value arise from the 4f polarization and charge transfer (CT) from the 3d metal ion. Besides the CT, the occupation of the 5d orbitals also arises from the local 4f → 5d orbital excitation. Though such type of excitations are forbidden in the Gd^{III} ion possessing spherical symmetry, this became allowed in a low-symmetry environment as witnessed earlier.[37] The σ-type $d_{x^2-y^2}$ orbital of the Cu^{II} ion promotes strong spin delocalization and renders a larger CT contribution to the 5d/6s/6p orbitals[47] of the lanthanides than the d_{xy} orbital of the V^{IV} ion. For complex

DOI: 10.1021/acs.inorgchem.6b01831
Inorg. Chem. 2016, 55, 11201−11215

1, no significant 3d-4f overlaps have been computed (see Table S20), while prominent NBO donor−acceptor interactions have been detected (14.36 and 7.19 kcal/mol in second-order perturbation theory analysis, see Table 2, S37 and Figure S8a-b) between the two centers. This reveals larger J_F contributions as compared to its J_{AF} counterpart, resulting in a ferromagnetic interaction between the two metal centers in complex **1**. This was pinpointed by the respective experimentalists[21b] through a deeper understanding of two competing exchange mechanisms as suggested earlier.[47] For complex **2** the d_{xy} orbital of the V^{IV} ion has significant interaction with the f_{xyz} orbital of the Dy^{III} ion leading to a significant J_{AF} contribution compared to complex **1**. This along with negligible charge transfer from the V^{IV} 3d orbital to the empty 5d orbitals of Dy^{III} ion leads to a very weak magnetic coupling for the V^{IV}−Dy^{III} pair. The empty 5d orbitals of the Tb^{III} in **3** possess larger orbital occupation than the Dy^{III} ions in **1**, and this is likely due to the stronger polarization of the 4f orbitals possessing six unpaired electrons. Besides, the J_{AF} contribution (see Tables 2, S20 and S37) is also found to be small compared to complex **1**, leading to a larger ferromagnetic interaction for the Cu^{II}−Tb^{III} pair. A very small exchange interaction estimated in **4** is attributed to smaller J_{AF} and J_F contributions. The prominent d_{xy}-f_{xyz} overlap of orbitals observed for the V^{IV}−Dy^{III} pair is absent here, and this leads to a very small J value (see Tables 2, S20 and S37). Spin density (see Figures 3c and S6) and NBO analysis (see Tables 2, S20 and S37) reveal a larger J_F and smaller J_{AF} term for complex **5**, suggesting dominant ferromagnetic coupling for the Cu^{II}−Ho^{III} pair. For complex **6** on the other hand, the d_{xy} orbital of V^{IV} overlaps significantly with some of the 4f orbitals leading to an enhanced J_{AF} contribution and net antiferromagnetic interaction. The ferro-antiferromagentic interactions observed for complexes **7** and **8** are found to be associated with $d_{x^2-y^2}$-4f and d_{xy}-4f orbital overlap with the later contributing significantly for the J_{VEr} coupling (see Tables 2, S20 and S37). Because of these reasons, all the LnCu complexes are strongly coupled and are ferromagnetic in nature compared to the analogous LnV complexes (see Table 1). Among the four LnV complexes studied, two complexes exhibit extremely weak ferromagnetic interaction (+0.15 cm^{-1} being the maximum observed for complex **2**) and other two complexes exhibit weak antiferromagnetic interaction, and this is generally due to less efficient CT and hence a reduced J_F contribution. Among the LnCu series studied, the following trend for the J's is observed TbCu (**3**) > DyCu (**1**) > HoCu (**5**) > ErCu (**7**), and this is the same as that of the number of unpaired electrons present in the 4f orbital. As the number of unpaired electrons are decreasing as we move from Tb to Er, the occupation in the formally empty 5d/6s/6p orbitals due to polarization of the 4f orbitals also decreases. This leads to less J_F contribution as we move from Tb to Er leading to a decrease in J values. We would like to pinpoint that as the number of unpaired electrons on the 4f-orbital increases, the number of overlap between the $d_{x^2-y^2}$ orbital of Cu^{II} and the magnetic orbitals of 4f shell also increases. This leads to an enhanced J_{AF} contribution as we move from Tb to Er. However, due to the axial nature of the $d_{x^2-y^2}$ orbital, all the overlap values computed are small leading to a very small J_{AF} contribution for all the complexes. The magnitude of the Mulliken spin population has been predicted to be slightly larger than the number of unpaired electrons in respective Ln^{III} ions (5.01, 6.03, 4.01, and 2.12 for for Dy^{III}, Tb^{III}, Ho^{III}, and Er^{III} ions, respectively). The Cu^{II} ion has has a spin density of ∼0.65 suggesting dominant spin delocalization,

Table 2. Second Order Perturbation Theory NBO Analysis on Complexes 1 and 3

Complex **1**		
donor NBO	acceptor NBO	CT interaction (kcal/mol)
Cu(s = 99.33%, d = 0.65%)	Dy(p = 57.72%, d = 34.36%, s = 7.83%)	7.19
Cu(s = 99.33%, d = 0.65%)	Dy(s = 50.45%, d = 40.63%, p = 8.88%)	2.28
Cu(s = 99.33%, d = 0.65%)	Dy(d = 64.77%, s = 34.81%, p = 0.33%)	2.21
Dy(s = 50.45%, d = 40.63%, p = 8.88%)	Cu(s = 80.34%, p = 12.89%, d = 6.77%)	14.36
Dy(d = 64.77%, s = 34.81%, p = 0.33%)	Cu(s = 80.34%, p = 12.89%, d = 6.77%)	5.47
Dy(p = 57.72%, d = 34.36%, s = 7.83%)	Cu(s = 80.34%, p = 12.89%, d = 6.77%)	5.12
Complex **3**		
donor NBO	acceptor NBO	CT interaction (kcal/mol)
Cu(s = 99.33%, d = 0.65%)	Tb(d = 72.59%, s = 27.11%)	7.03
Cu(s = 99.33%, d = 0.65%)	Tb(s = 56.97%, d = 34.37%)	2.32
Cu(s = 99.33%, d = 0.65%)	Tb(p = 75.69%, d = 13.80%, s = 10.48%)	2.05
Cu(s = 100%)	Tb(p = 75.69%, d = 13.80%, s = 10.48%)	1.18
Tb(d = 72.59%, s = 27.11%)	Cu(s = 77.46%, p = 15.41%, d = 7.13%)	21.60
Tb(s = 56.97%, d = 34.37%, p = 8.62%)	Cu(s = 77.46%, p = 15.41%, d = 7.13%)	8.90
Tb(p = 75.69%, d = 13.80%, s = 10.48%)	Cu(s = 77.46%, p = 15.41%, d = 7.13%)	3.53

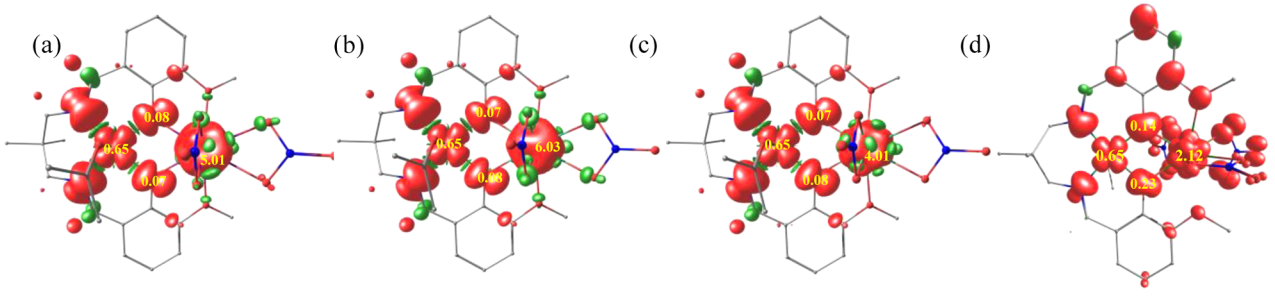

Figure 6. DFT computed spin density plots for complexes (a) **1**, (b) **3**, (c) **5**, and (d) **7**. Red and green surfaces are positive and negative regions respectively, and H elements have been removed for clarity. The isodensity surface represented corresponds to a value of 0.005 $e^-/bohr^3$.

DOI: 10.1021/acs.inorgchem.6b01831
Inorg. Chem. 2016, 55, 11201−11215

while V^{IV} ion has a spin density of ~1.18 suggesting spin polarization mechanisms (see Figure 6 and S6 in Supporting Information). Spin density on the Cu^{II} center of complex **3** remains the same as that of complex **1** revealing a fact that it does not play a role in enhancing the J_F contribution via charge transfer. However, the empty 5d orbitals of the Tb^{III} possess larger orbital occupation than the Dy^{III} ions in **1**, and this is likely due to the stronger polarization of the 4f orbitals possessing six unpaired electrons. Besides, the J_{AF} contribution (see Tables 2, S20 and S37) is also found to be small compared to complex **1** leading to a larger ferromagnetic interaction for the Cu^{II}–Tb^{III} pair.

Influence of Magnetic Coupling in Magnetization Relaxation. Both the computed J values and the POLY_ANISO[44] computed blockade barriers need to be analyzed in order to comprehend the impact of magnetic coupling on the magnetization relaxation. Among the LnCu analogous, TbCu (complex **3**) shows the largest (+5.3 cm^{-1}) exchange interaction between Tb^{III} and Cu^{II} ions, while the second best is estimated to be the DyCu complex. Coincidently, both these complexes exhibit SMM behavior with TbCu exhibiting a much larger barrier height than the DyCu complex. This postulates that the magnetic exchange certainly influences the magnetization relaxation soliciting stronger {3d-4f} interactions to obtain better SMM characteristics. The exchange interaction is found to suppress the QTM between the ground states and thus enhances the chance to observe SMM characteristics {for complexes **1** and **3** the estimated U_{eff} (U_{cal}) values are 7.99 (4.2) cm^{-1}, 29.4 (15.7) cm^{-1}, respectively}. The transversal moment matrix element pertinent to QTM for TbCu complex is considerable (0.02 μ_B), while tunnel splitting of DyCu is also non-negligible (0.05 cm^{-1}). The tunnel splitting estimated for the Tb^{III} single-ion behavior is 0.31 cm^{-1}, suggesting significant tunnelling, and thus SMM behavior is not expected. The introduction of a Cu^{II} ion induces a significant exchange interaction which quenches the QTM to a certain extent (0.02 μ_B and Δ_{tun} = 4.2 × 10^{-7} cm^{-1}) and offers a barrier height of 15.7 cm^{-1} for the magnetization blockade. Thus, exchange interaction plays a constructive role here. For DyCu complex, the transversal magnetic moment corresponding to a QTM pathway between the m_J = ± 15/2 is computed to be 0.05 μ_B, while upon introduction of Cu^{II} ion, the tunnel splitting is estimated to be 0.05 cm^{-1}. Here no significant improvement is detected, in fact because of the exchange interaction the first excited state is deduced to lie at 4.2 cm^{-1}, while single-ion Dy^{III} possesses the first excited state at 60 cm^{-1}, suggesting the fact that exchange does not help to improve the behavior and a diamagnetic ion such as Zn^{II} in place of Cu^{II} would have offered better SMM characteristics as has been witnessed earlier by us and others.[19b,24b,34]

For DyV complex on the other hand, the ground KD QTM is very significant (0.21 μ_B) based on single-ion analysis. The exchange interaction quenches this behavior, and for the exchange coupled states (see Figure 7b), the tunnel splitting is estimated to be 0.01 cm^{-1}. Although the overall effect here is constructive, the exchange interaction is too small to offer a reasonable blockade barrier. For TbV complex as well significant improvement to QTM is witnessed for the exchange-coupled states {1.13 cm^{-1} as Δ_{tun} vs 0.59 μ_B (pertinent magnetic moment matrix element) for single-ion vs TbV exchange coupled state}. A very small exchange and stronger mixing lead to near isotropic g-values for the exchange-coupled state, and thus no SMM behavior is expected.

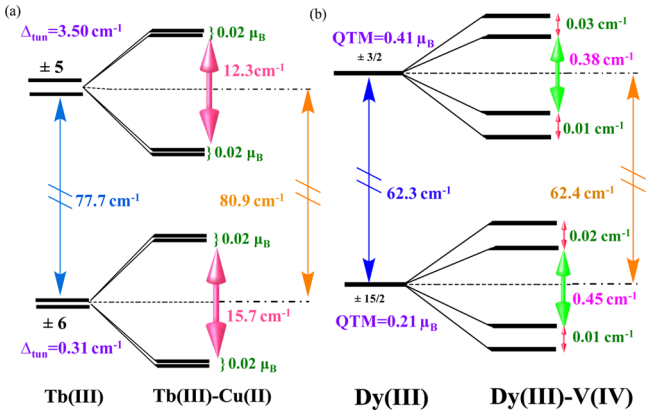

Figure 7. Diagram explaining the splitting of ± m_J levels in Dy^{III} and Tb^{III} centers in complexes **3** and **2** respectively. This is followed by their subsequent splitting of energy levels on coupling with transition metal ions V^{IV} and Cu^{II} respectively. [Note: QTM is generally represented in μ_B unit and tunnel splitting is denoted by cm^{-1} unit.]

For HoCu complex although the estimated exchange interaction is moderate (+1.05 cm^{-1}), a larger matrix element corresponding to the QTM process (0.72 μ_B), significant transverse anisotropy, and strong mixing of m_J levels at the ground state lead to the absence of SMM behavior (g_{zz} = 8.66, g_{xx} = 2.06, and g_{yy} = 2.26). For ErCu complex the estimated J value is the smallest ferromagnetic exchange interactions among the LnCu complexes (J = +0.24 cm^{-1}). Smaller exchange induces significant tunnel splitting (0.01 cm^{-1}), and the first excited state is found to lie merely at 0.27 cm^{-1} higher in energy leading to the absence of SMM behavior. All the LnV complexes show very weak exchange interaction leading to very close lying excited states and thus offer negligible blockade barriers.

Magnetostructural Correlations: Single-Ion Anisotropy vs the Exchange Interaction. As exchange interaction is found to play a decisive role in deciphering the SMM behavior as well as the barrier height for magnetization blockade, we have developed a magneto-structural correlation by varying the Dy–O–O–Cu dihedral angle (butterfly angle) in the full structure of complex **1**. In analogous GdCu complexes, the Gd–O–Cu–O[33f]/Gd–O–O–Cu[40] and DyCu complexes, Dy–O–O–Cu[46] butterfly angle has been found to influence the exchange interaction significantly, driving us to select this parameter for our study. Besides the dihedral angle (φ) is also found to marginally differ among complexes **1**–**8** studied (17.4 ± 0.1° for complexes **1**, **3**, **5**, and **7**; and 21.1 ± 0.2° for complexes **2** ,**4**, **6**, and **8**). The developed correlation along with J_{CuDy} estimated using BS-DFT and U_{cal} estimated from SINGLE_ANISO[45] is given in Figure 8.

As predicted earlier, smaller dihedral angles are found to increase the J_{CuDy} values, and the graph reveals a near linear relationship between the J_{CuDy} and the φ parameter. This is consistent with the experimental correlations developed recently for a series of {CuDy} complexes.[46] However, to our surprise, the U_{cal} values are found to decrease with a decrease in the φ parameter, and this antagonizing behavior between the J_{CuDy} and the U_{cal} reveals how complex the nature of magnetic relaxation is in these {3d-4f} SMMs. As the Dy–O–O–Cu dihedral is varied, this induces a significant distortion around the Dy^{III} coordination sphere leading to a dramatic decrease in the U_{cal} values. This illustrates how subtle the spin Hamiltonian parameters are in {3d-4f} SMMs, and extensive experimental

DOI: 10.1021/acs.inorgchem.6b01831
Inorg. Chem. 2016, 55, 11201–11215

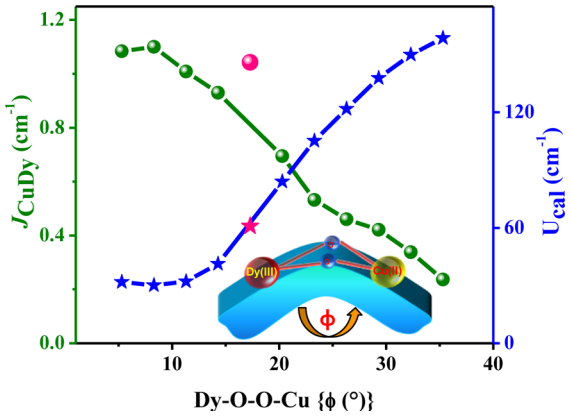

Figure 8. Magnetostructural correlations performed on complex **1** to investigate the effect of the Dy−O−O−Cu dihedral angle (φ) on the J_{CuDy} exchange and the Dy^{III} U_{cal} values.

and theoretical studies are required for achieving new generation {3d-4f} SMMs.

Role of Covalency in Magnetic Coupling and the U_{cal} Values. It is known that in the transition metal dimers substitution of the oxygen atom by a more covalent sulfur atom would enhance the exchange coupling.[38] Besides there is also an experimental report on several Dy-chalcogenide complexes exhibiting SMM behavior.[39] To see if the exchange interaction increases, we have created fictitious model complexes where both the bridging oxygen atoms and the methoxy oxygen atoms in the ligand moiety are substituted by the sulfur atom for complexes **1** and **3** (see Figures S4−S5 in Supporting Information, models **I** and **II** respectively). The BS-DFT calculations estimate the exchange coupling as +9.3 cm^{-1} (see Table S38) for the sulfur model against +1.1 cm^{-1} obtained for the original structure. Similarly for complex **3**, +10.9 cm^{-1} (see Table S39) exchange coupling has been observed. These estimated exchange interactions are 10 times larger than that found for oxygen analogue; however, the single-ion anisotropy is also found to be significantly influenced by this substitution. The ground state anisotropy for the substituted systems becomes non-axial with g_{xx} = 11.54, g_{yy} = 7.03, and g_{zz} = 0.88, and the wave function analysis demonstrates that the ground state of the Dy^{III} ion in this complex is a mixture of $|\pm 3/2\rangle$, $|\pm 1/2\rangle$ and $|\pm 7/2\rangle$ (47%$|\pm 3/2\rangle$+26%$|\pm 1/2\rangle$+24%$|\pm 7/2\rangle$) state leading to a significant QTM process (3.10 μ_B). Besides the first excited level is computed to lie at 29.7 cm^{-1}, and this also sees a drastic reduction compared to the oxygen analogue. Similarly for complex **3** model structure, the tunnel splitting is estimated to be very high (0.31 vs 4.43 cm^{-1}). This is necessarily due to the notion that the sulfur being more covalent than oxygen mixes much more strongly with the 4f-orbitals leading to a drastic reduction on single-ion behavior. Although the exchange coupling is significantly enhanced, this is accompanied by the concomitant reduction in the single-ion anisotropy.

5. CONCLUSIONS

In this study, using a DFT and ab initio methodology we have studied eight structurally analogous {3d-4f} complexes to assess the Lines model popularly employed to extract the exchange coupling constant. The computed value is in agreement with the experimental data offering confidence in the employed methodology. Among complexes **1**−**8**, complexes **1** and **3** are found to exhibit SMM behavior. This is attributed to the strong ferromagnetic exchange computed for these two complexes. For other complexes, the J values are found to be very small leading to the absence of SMM behavior. Our calculations yield the following order for the J values: **3** > **1** > **5** > **7** > **2** > **4** > **8** > **6**. Among the LnCu analogous, the exchange value decreases in the same order as number of unpaired electrons (TbCu > DyCu > HoCu > ErCu). We can conclude that, stronger exchange interaction is correlated to weaker single-ion anisotropy. This is reminiscent of an earlier[4b] established fact that, spin (S) and magnetic anisotropy (D) are inversely proportional to each other.

We have developed a mechanism of magnetic coupling for anisotropic {3d-4f} pair where empty 5d/6s/6p orbitals are found to play an important role in determining the sign and strength of J values. The magneto-structural correlations developed a postulate that the targeted structural distortions to achieve larger J's as done conventionally in transition metal dimers are very challenging here as the structural distortion significantly influences the single-ion anisotropy. Particularly our correlation developed on DyCu complex based on the Dy−O−O−Cu dihedral angle reveals that large J's and large single-ion behavior are unlikely to coexist as desired.

To this end, here for the first time we have attempted to understand the role of magnetic exchange interaction in the magnetization relaxation of structurally analogous {3d-4f} complexes. Our study suggests that both the single-ion anisotropy and the exchange interactions need to be targeted simultaneously to achieve new generation {3d-4f} SMMs.

■ ASSOCIATED CONTENT

Supporting Information

The Supporting Information is available free of charge on the ACS Publications website at DOI: 10.1021/acs.inorgchem.6b01831.

CASSCF+RASSI-SO computed spin-free and spin−orbit energies for complexes **1**−**8**; energies of all the low-lying KDs, along with the computed g-anisotropies for complexes **1**−**8**; orientation of the computed ground KD g anisotropy for complexes **2**, **7**, and **8** (Figure S1); energies and g tensors of the lowest exchange doublets for complexes **1**−**8**; computed overlap integrals for complexes **1**−**8** (see Table S20); BS-DFT computed exchange (J) interactions for complexes **1**−**8** (Table S19); donor−acceptor charge transfer interaction for complexes **1**−**8** (Table 2, S37 and Figure S8); ab initio computed ground state anisotropy orientation with respect to its corresponding electrostatic anisotropy axis (Figure S2); ground state g tensor orientations for all the Ln(III) ions superposed in DyCu complex (Figure S3); energies of all the low-lying KDs, along with the computed g-anisotropies for S substituted models (**I** and **II** of complexes **1** and **3** respectively, Tables S38 and S39) with their orientations (Figures S4−S5); DFT computed HS geometry spin density for complexes **2**, **4**, **6**, and **8** (Figure S6); ab initio computed crystal field parameters for complexes **1**−**8** (Table S18) (PDF)

■ AUTHOR INFORMATION

Corresponding Author

*Phone: +91-22-2576 7183. Fax: +91-22-2576 7152. E-mail: rajaraman@chem.iitb.ac.in.

DOI: 10.1021/acs.inorgchem.6b01831
Inorg. Chem. 2016, 55, 11201−11215

Notes

The authors declare no competing financial interest.

■ ACKNOWLEDGMENTS

G.R. would like to acknowledge the financial support from the Government of India through the Department of Science and Technology (EMR/2014/000247) and the generous computational resources from Indian Institute of Technology-Bombay. T.G. thanks UGC for a SRF fellowship. M.F.B. is indebted to IIT Bombay. We would like to express our sincere gratitude to Dr. Liviu Ungur, KU, Leuven, Belgium, for providing us the SINGLE_ANISO[45] and POLY_ANISO[44] code for our computational study.

■ REFERENCES

(1) (a) Wernsdorfer, W.; Bhaduri, S.; Boskovic, C.; Christou, G.; Hendrickson, D. N. Spin-parity dependent tunneling of magnetization in single-molecule magnets. *Phys. Rev. B: Condens. Matter Mater. Phys.* **2002**, *65*, 180403. (b) Ruiz, E.; Alvarez, S.; Rodriguez-Fort, A.; Alemany, P.; Pouillon, Y.; Massobrio, A. In *Magnetism: Molecules to Materials*; Miller, J. S., Drillon, M., Ed.; Wiley-VCH: Weinheim, 2001; Vol. *II*, pp 227. (c) Christou, G.; Gatteschi, D.; Hendrickson, D. N.; Sessoli, R. Single-molecule magnets. *MRS Bull.* **2000**, *25*, 66. (d) Gatteschi, D.; Caneschi, A.; Pardi, L.; Sessoli, R. Large Clusters of Metal-Ions - the Transition from Molecular to Bulk Magnets. *Science* **1994**, *265*, 1054. (e) Sessoli, R.; Tsai, H. L.; Schake, A. R.; Wang, S. Y.; Vincent, J. B.; Folting, K.; Gatteschi, D.; Christou, G.; Hendrickson, D. N. High-Spin Molecules - $[Mn_{12}O_{12}(O_2Cr)16(H_2O)_4]$. *J. Am. Chem. Soc.* **1993**, *115*, 1804. (f) Sessoli, R.; Gatteschi, D.; Caneschi, A.; Novak, M. A. Magnetic bistability in a metal-ion cluster. *Nature* **1993**, *365*, 141. (g) Kahn, O. In *Molecular Magnetism*; VCH Publishers, Inc.: Orsay, France, 1993.

(2) (a) Aromi, G.; Aguila, D.; Gamez, P.; Luis, F.; Roubeau, O. Design of magnetic coordination complexes for quantum computing. *Chem. Soc. Rev.* **2012**, *41*, 537. (b) Sanvito, S. Molecular spintronics. *Chem. Soc. Rev.* **2011**, *40*, 3336. (c) Winpenny, R. E. P. Quantum Information Processing Using Molecular Nanomagnets As Qubits. *Angew. Chem., Int. Ed.* **2008**, *47*, 7992. (d) Roch, N.; Florens, S.; Bouchiat, V.; Wernsdorfer, W.; Balestro, F. Quantum phase transition in a single-molecule quantum dot. *Nature* **2008**, *453*, 633. (e) Bogani, L.; Wernsdorfer, W. Molecular spintronics using single-molecule magnets. *Nat. Mater.* **2008**, *7*, 179. (f) Hill, S.; Edwards, R. S.; Aliaga-Alcalde, N.; Christou, G. Quantum coherence in an exchange-coupled dimer of single-molecule magnets. *Science* **2003**, *302*, 1015. (g) Leuenberger, M. N.; Loss, D. Quantum computing in molecular magnets. *Nature* **2001**, *410*, 789. (h) Wernsdorfer, W.; Sessoli, R. Quantum Phase Interference and Parity Effects in Magnetic Molecular Clusters. *Science* **1999**, *284*, 133.

(3) (a) Chilton, N. F. Design Criteria for High-Temperature Single-Molecule Magnets. *Inorg. Chem.* **2015**, *54*, 2097. (b) Ungur, L.; Le Roy, J. J.; Korobkov, I.; Murugesu, M.; Chibotaru, L. F. Fine-tuning the Local Symmetry to Attain Record Blocking Temperature and Magnetic Remanence in a Single-Ion Magnet. *Angew. Chem., Int. Ed.* **2014**, *53*, 4413. (c) Le Roy, J. J.; Korobkov, I.; Kim, J. E.; Schelter, E. J.; Murugesu, M. Structural and magnetic conformation of a cerocene $[Ce(COT'')_2]^-$ exhibiting a uniconfigurational f^1 ground state and slow-magnetic relaxation. *Dalton Trans.* **2014**, *43*, 2737. (d) Langley, S. K.; Wielechowski, D. P.; Vieru, V.; Chilton, N. F.; Moubaraki, B.; Abrahams, B. F.; Chibotaru, L. F.; Murray, K. S. A $\{(Cr_2Dy_2^{III})\text{-}Dy^{III}\}$ Single-Molecule Magnet: Enhancing the Blocking Temperature through 3d Magnetic Exchange. *Angew. Chem., Int. Ed.* **2013**, *52*, 12014. (e) Rinehart, J. D.; Fang, M.; Evans, W. J.; Long, J. R. A N_2^{3-} Radical-Bridged Terbium Complex Exhibiting Magnetic Hysteresis at 14 K. *J. Am. Chem. Soc.* **2011**, *133*, 14236.

(4) (a) Parois, P.; Moggach, S. A.; Sanchez-Benitez, J.; Kamenev, K. V.; Lennie, A. R.; Warren, J. E.; Brechin, E. K.; Parsons, S.; Murrie, M. Pressure-induced Jahn-Teller switching in a Mn_{12} nanomagnet. *Chem. Commun.* **2010**, *46*, 1881. (b) Ruiz, E.; Cirera, J.; Cano, J.; Alvarez, S.; Loose, C.; Kortus, J. Can large magnetic anisotropy and high spin really coexist? *Chem. Commun.* **2008**, 52. (c) Milios, C. J.; Vinslava, A.; Wernsdorfer, W.; Moggach, S.; Parsons, S.; Perlepes, S. P.; Christou, G.; Brechin, E. K. A record anisotropy barrier for a single-molecule magnet. *J. Am. Chem. Soc.* **2007**, *129*, 2754. (d) Sañudo, E. C.; Wernsdorfer, W.; Abboud, K. A.; Christou, G. Synthesis, Structure, and Magnetic Properties of a Mn21 Single-Molecule Magnet. *Inorg. Chem.* **2004**, *43*, 4137. (e) Brechin, E. K.; Boskovic, C.; Wernsdorfer, W.; Yoo, J.; Yamaguchi, A.; Sañudo, E. C.; Concolino, T. R.; Rheingold, A. L.; Ishimoto, H.; Hendrickson, D. N.; Christou, G. Quantum Tunneling of Magnetization in a New [Mn18]2+ Single-Molecule Magnet with S = 13. *J. Am. Chem. Soc.* **2002**, *124*, 9710.

(5) Ako, A. M.; Hewitt, I. J.; Mereacre, V.; Clérac, R.; Wernsdorfer, W.; Anson, C. E.; Powell, A. K. A Ferromagnetically Coupled Mn19 Aggregate with a Record S = 83/2 Ground Spin State. *Angew. Chem., Int. Ed.* **2006**, *45*, 4926.

(6) Zadrozny, J. M.; Xiao, D. J.; Atanasov, M.; Long, G. J.; Grandjean, F.; Neese, F.; Long, J. R. Magnetic blocking in a linear iron(I) complex. *Nat. Chem.* **2013**, *5*, 577.

(7) (a) Zadrozny, J. M.; Atanasov, M.; Bryan, A. M.; Lin, C.-Y.; Rekken, B. D.; Power, P. P.; Neese, F.; Long, J. R. Slow magnetization dynamics in a series of two-coordinate iron(ii) complexes. *Chem. Sci.* **2013**, *4*, 125. (b) Yang, F.; Zhou, Q.; Zhang, Y.; Zeng, G.; Li, G.; Shi, Z.; Wang, B.; Feng, S. Inspiration from old molecules: field-induced slow magnetic relaxation in three air-stable tetrahedral cobalt(ii) compounds. *Chem. Commun.* **2013**, *49*, 5289. (c) Zadrozny, J. M.; Liu, J.; Piro, N. A.; Chang, C. J.; Hill, S.; Long, J. R. Slow magnetic relaxation in a pseudotetrahedral cobalt(ii) complex with easy-plane anisotropy. *Chem. Commun.* **2012**, *48*, 3927.

(8) (a) Zeng, D.; Ren, M.; Bao, S.-S.; Feng, J.-S.; Li, L.; Zheng, L.-M. pH-controlled polymorphism in a layered dysprosium phosphonate and its impact on the magnetization relaxation. *Chem. Commun.* **2015**, *51*, 2649. (b) Rosado Piquer, L. R.; Sanudo, E. C. Heterometallic 3d-4f single-molecule magnets. *Dalton Trans.* **2015**, *44*, 8771. (c) Zhang, P.; Guo, Y. N.; Tang, J. K. Recent advances in dysprosium-based single molecule magnets: Structural overview and synthetic strategies. *Coord. Chem. Rev.* **2013**, *257*, 1728. (d) Woodruff, D. N.; Winpenny, R. E. P.; Layfield, R. A. Lanthanide Single-Molecule Magnets. *Chem. Rev.* **2013**, *113*, 5110. (e) Meihaus, K. R.; Long, J. R. Magnetic blocking at 10 K and a Dipolar-mediated avalanche in salts of the bis(η8-cyclo-octatetraenide) complex $[Er(COT)_2]^-$. *J. Am. Chem. Soc.* **2013**, *135*, 17952. (f) Habib, F.; Murugesu, M. Lessons learned from dinuclear lanthanide nano-magnets. *Chem. Soc. Rev.* **2013**, *42*, 3278. (g) Chilton, N. F.; Langley, S. K.; Moubaraki, B.; Soncini, A.; Batten, S. R.; Murray, K. S. Single molecule magnetism in a family of mononuclear beta-diketonate lanthanide(III) complexes: rationalization of magnetic anisotropy in complexes of low symmetry. *Chem. Sci.* **2013**, *4*, 1719. (h) Chilton, N. F.; Collison, D.; McInnes, E. J. L.; Winpenny, R. E. P.; Soncini, A. An electrostatic model for the determination of magnetic anisotropy in dysprosium complexes. *Nat. Commun.* **2013**, *4*, 2551. (i) Sorace, L.; Benelli, C.; Gatteschi, D. Lanthanides in molecular magnetism: old tools in a new field. *Chem. Soc. Rev.* **2011**, *40*, 3092. (j) Sessoli, R.; Powell, A. K. Strategies towards single molecule magnets based on lanthanide ions. *Coord. Chem. Rev.* **2009**, *253*, 2328. (k) Ishikawa, N.; Sugita, M.; Ishikawa, T.; Koshihara, S.; Kaizu, Y. Lanthanide double-decker complexes functioning as magnets at the single-molecular level. *J. Am. Chem. Soc.* **2003**, *125*, 8694.

(9) (a) Binnemans, K. Lanthanide-Based Luminescent Hybrid Materials. *Chem. Rev.* **2009**, *109*, 4283. (b) Ward, M. D. Transition-metal sensitised near-infrared luminescence from lanthanides in d–f heteronuclear arrays. *Coord. Chem. Rev.* **2007**, *251*, 1663. (c) Charbonnière, L.; Ziessel, R.; Guardigli, M.; Roda, A.; Sabbatini, N.; Cesario, M. Lanthanide Tags for Time-Resolved Luminescence Microscopy Displaying Improved Stability and Optical Properties. *J. Am. Chem. Soc.* **2001**, *123*, 2436.

(10) (a) Binnemans, K.; Gschneidner, K. A., Jr.; Bünzli, J.-C. G.; Pecharsky, V. K. In *Handbook on the Physics and Chemistry Lanthanides of Rare-Earth*; Elsevier: Amsterdam, The Netherlands, 2005; Vol. 35,

DOI: 10.1021/acs.inorgchem.6b01831
Inorg. Chem. 2016, 55, 11201–11215

pp107. (b) Osa, S.; Kido, T.; Matsumoto, N.; Re, N.; Pochaba, A.; Mrozinski, J. A tetranuclear 3d-4f single molecule magnet: [(CuLTbIII)-L-II(hfac)(2)](2). *J. Am. Chem. Soc.* **2004**, *126*, 420.

(11) (a) Caneschi, A.; Gatteschi, D.; Sessoli, R.; Barra, A. L.; Brunel, L. C.; Guillot, M. Alternating current susceptibility, high field magnetization, and millimeter band EPR evidence for a ground S = 10 state in [Mn12O12(Ch3COO)16(H2O)4].2CH3COOH.4H2O. *J. Am. Chem. Soc.* **1991**, *113*, 5873. (b) Boyd, P. D. W.; Li, Q.; Vincent, J. B.; Folting, K.; Chang, H. R.; Streib, W. E.; Huffman, J. C.; Christou, G.; Hendrickson, D. N. Potential building blocks for molecular ferromagnets: [Mn12O12(O2CPh)16(H2O)4] with a S = 14 ground state. *J. Am. Chem. Soc.* **1988**, *110*, 8537.

(12) Rinehart, J. D.; Long, J. R. Exploiting single-ion anisotropy in the design of f-element single-molecule magnets. *Chem. Sci.* **2011**, *2*, 2078.

(13) (a) Blagg, R. J.; Ungur, L.; Tuna, F.; Speak, J.; Comar, P.; Collison, D.; Wernsdorfer, W.; McInnes, E. J. L.; Chibotaru, L. F.; Winpenny, R. E. P. Magnetic relaxation pathways in lanthanide single-molecule magnets. *Nat. Chem.* **2013**, *5*, 673. (b) Boulon, M. E.; Cucinotta, G.; Luzon, J.; Degl'Innocenti, C.; Perfetti, M.; Bernot, K.; Calvez, G.; Caneschi, A.; Sessoli, R. Magnetic Anisotropy and Spin-Parity Effect Along the Series of Lanthanide Complexes with DOTA. *Angew. Chem., Int. Ed.* **2013**, *52*, 350. (c) Jung, J.; da Cunha, T. T.; Le Guennic, B.; Pointillart, F.; Pereira, C. L. M.; Luzon, J.; Golhen, S.; Cador, O.; Maury, O.; Ouahab, L. Magnetic Studies of Redox-Active Tetrathiafulvalene-Based Complexes: Dysprosium vs. Ytterbium Analogues. *Eur. J. Inorg. Chem.* **2014**, *2014*, 3888.

(14) Langley, S. K.; Chilton, N. F.; Moubaraki, B.; Murray, K. S. Single-Molecule Magnetism in Three Related {CoIII2DyIII2}-Acetylacetonate Complexes with Multiple Relaxation Mechanisms. *Inorg. Chem.* **2013**, *52*, 7183.

(15) Guo, Y. N.; Xu, G. F.; Wernsdorfer, W.; Ungur, L.; Guo, Y.; Tang, J. K.; Zhang, H. J.; Chibotaru, L. F.; Powell, A. K. Strong Axiality and Ising Exchange Interaction Suppress Zero-Field Tunneling of Magnetization of an Asymmetric Dy-2 Single-Molecule Magnet. *J. Am. Chem. Soc.* **2011**, *133*, 11948.

(16) Wernsdorfer, W.; Aliaga-Alcalde, N.; Hendrickson, D. N.; Christou, G. Exchange-biased quantum tunnelling in a supramolecular dimer of single-molecule magnets. *Nature* **2002**, *416*, 406.

(17) (a) Ganivet, C. R.; Ballesteros, B.; de la Torre, G.; Clemente-Juan, J. M.; Coronado, E.; Torres, T. Influence of Peripheral Substitution on the Magnetic Behavior of Single-Ion Magnets Based on Homo- and Heteroleptic TbIII Bis(phthalocyaninate). *Chem. - Eur. J.* **2013**, *19*, 1457. (b) Rinehart, J. D.; Fang, M.; Evans, W. J.; Long, J. R. Strong exchange and magnetic blocking in N-2(3-)-radical-bridged lanthanide complexes. *Nat. Chem.* **2011**, *3*, 538. (c) Murrie, M. Cobalt(ii) single-molecule magnets. *Chem. Soc. Rev.* **2010**, *39*, 1986.

(18) (a) Langley, S. K.; Wielechowski, D. P.; Vieru, V.; Chilton, N. F.; Moubaraki, B.; Chibotaru, L. F.; Murray, K. S. Modulation of slow magnetic relaxation by tuning magnetic exchange in {Cr2Dy2} single molecule magnets. *Chem. Sci.* **2014**, *5*, 3246. (b) Mondal, K. C.; Sundt, A.; Lan, Y.; Kostakis, G. E.; Waldmann, O.; Ungur, L.; Chibotaru, L. F.; Anson, C. E.; Powell, A. K. Coexistence of distinct single-ion and exchange-based mechanisms for blocking of magnetization in a Co(II)2Dy(III)2 single-molecule magnet. *Angew. Chem., Int. Ed.* **2012**, *51*, 7550.

(19) (a) Li, X.-L.; Min, F.-Y; Wang, C.; Lin, S.-Y.; Liu, Z.; Tang, J. Utilizing 3d−4f Magnetic Interaction to Slow the Magnetic Relaxation of Heterometallic Complexes. *Inorg. Chem.* **2015**, *54*, 4337. (b) Ruiz, J.; Lorusso, G.; Evangelisti, M.; Brechin, E. K.; Pope, S. J. A.; Colacio, E. Closely-Related ZnII2LnIII2 Complexes (LnIII = Gd, Yb) with Either Magnetic Refrigerant or Luminescent Single-Molecule Magnet Properties. *Inorg. Chem.* **2014**, *53*, 3586. (c) Ruamps, R.; Batchelor, L. J.; Guillot, R.; Zakhia, G.; Barra, A.-L.; Wernsdorfer, W.; Guihery, N.; Mallah, T. Ising-type magnetic anisotropy and single molecule magnet behaviour in mononuclear trigonal bipyramidal Co(ii) complexes. *Chem. Sci.* **2014**, *5*, 3418. (d) Langley, S. K.; Ungur, L.; Chilton, N. F.; Moubaraki, B.; Chibotaru, L. F.; Murray, K. S. Single-Molecule Magnetism in a Family of {CoIII2DyIII2} Butterfly Complexes: Effects of Ligand Replacement on the Dynamics of Magnetic Relaxation. *Inorg. Chem.* **2014**, *53*, 4303. (e) Feltham, H. L. C.; Brooker, S. Review of purely 4f and mixed-metal nd-4f single-molecule magnets containing only one lanthanide ion. *Coord. Chem. Rev.* **2014**, *276*, 1. (f) Langley, S. K.; Chilton, N. F.; Moubaraki, B.; Murray, K. S. Anisotropy barrier enhancement via ligand substitution in tetranuclear {CoIII2LnIII2} single molecule magnets. *Chem. Commun.* **2013**, *49*, 6965. (g) Langley, S. K.; Chilton, N. F.; Ungur, L.; Moubaraki, B.; Chibotaru, L. F.; Murray, K. S. Heterometallic Tetranuclear [Ln(2)(III)Co(2)(III)] Complexes Including Suppression of Quantum Tunneling of Magnetization in the [(Dy2Co2III)-Co-III] Single Molecule Magnet. *Inorg. Chem.* **2012**, *51*, 11873. (h) Rinck, J.; Novitchi, G.; Van den Heuvel, W.; Ungur, L.; Lan, Y.; Wernsdorfer, W.; Anson, C. E.; Chibotaru, L. F.; Powell, A. K. An Octanuclear [CrIII4DyIII4] 3d−4f Single-Molecule Magnet. *Angew. Chem., Int. Ed.* **2010**, *49*, 7583. (i) Karotsis, G.; Kennedy, S.; Teat, S. J.; Beavers, C. M.; Fowler, D. A.; Morales, J. J.; Evangelisti, M.; Dalgarno, S. J.; Brechin, E. K. [MnIII4LnIII4] Calix[4]arene Clusters as Enhanced Magnetic Coolers and Molecular Magnets. *J. Am. Chem. Soc.* **2010**, *132*, 12983. (j) Novitchi, G.; Wernsdorfer, W.; Chibotaru, L. F.; Costes, J. P.; Anson, C. E.; Powell, A. K. Supramolecular "Double-Propeller" Dimers of Hexanuclear Cu-II/Ln(III) Complexes: A-{Cu3Dy3}(2) Single-Molecule Magnet. *Angew. Chem., Int. Ed.* **2009**, *48*, 1614. (k) Pointillart, F.; Bernot, K.; Sessoli, R.; Gatteschi, D. Effects of 3d−4f Magnetic Exchange Interactions on the Dynamics of the Magnetization of DyIII-MII-DyIII Trinuclear Clusters. *Chem. - Eur. J.* **2007**, *13*, 1602. (l) Langley, S. K.; Wielechowski, D. P.; Vieru, V.; Chilton, N. F.; Moubaraki, B.; Abrahams, B. F.; Chibotaru, L. F.; Murray, K. S. A {(Cr2Dy2III)-Dy-III} Single-Molecule Magnet: Enhancing the Blocking Temperature through 3d Magnetic Exchange. *Angew. Chem., Int. Ed.* **2013**, *52*, 12014.

(20) Wu, J.; Zhao, L.; Zhang, P.; Zhang, L.; Guo, M.; Tang, J. Linear 3d-4f compounds: synthesis, structure, and determination of the d-f magnetic interaction. *Dalton Trans.* **2015**, *44*, 11935.

(21) (a) Tancini, E.; Mannini, M.; Sainctavit, P.; Otero, E.; Sessoli, R.; Cornia, A. On-Surface Magnetometry: The Evaluation of Superexchange Coupling Constants in Surface-Wired Single-Molecule Magnets. *Chem. - Eur. J.* **2013**, *19*, 16902. (b) Ishida, T.; Watanabe, R.; Fujiwara, K.; Okazawa, A.; Kojima, N.; Tanaka, G.; Yoshii, S.; Nojiri, H. Exchange coupling in TbCu and DyCu single-molecule magnets and related lanthanide and vanadium analogs. *Dalton Trans.* **2012**, *41*, 13609. (c) Hernando, A.; Kulik, T. Exchange interactions through amorphous paramagnetic layers in ferromagnetic nanocrystals. *Phys. Rev. B: Condens. Matter Mater. Phys.* **1994**, *49*, 7064. (d) Burger, J. P.; Vajda, P.; Daou, J. N.; Chouteau, G. Effect of hydrogen in solid solution upon the magnetic properties of monocrystalline erbium. *J. Phys. F: Met. Phys.* **1986**, *16*, 1275.

(22) (a) Rose, C.; Boulon, J.; Hervo, M.; Holmgren, H.; Asmi, E.; Ramonet, M.; Laj, P.; Sellegri, K. Long-term observations of cluster ion concentration, sources and sinks in clear sky conditions at the high-altitude site of the Puy de Dome, France. *Atmos. Chem. Phys.* **2013**, *13*, 11573. (b) Amoretti, G.; Caciuffo, R.; Carretta, S.; Guidi, T.; Magnani, N.; Santini, P. Inelastic neutron scattering investigations of molecular nanomagnets. *Inorg. Chim. Acta* **2008**, *361*, 3771. (c) Gudel, H. U.; Hauser, U.; Furrer, A. Electronic Ground-State Properties of Tetranuclear Hexa-Mu-Hydroxo-Bis(Tetraamminechromium(Iii))Bis-(Diamminechromium(Iii)) Chloride - Spectroscopic and Magneto-chemical Study. *Inorg. Chem.* **1979**, *18*, 2730.

(23) (a) Barra, A. L.; Gatteschi, D.; Sessoli, R.; Abbati, G. L.; Cornia, A.; Fabretti, A. C.; Uytterhoeven, M. G. Electronic structure of manganese(III) compounds from high-frequency EPR spectra. *Angew. Chem., Int. Ed. Engl.* **1997**, *36*, 2329. (b) Bencini, A.; Gatteschi, D. In *EPR of Exchange Coupled Systems*; Springer-Verlag: Berlin, 1990.

(24) (a) Das, C.; Upadhyay, A.; Vaidya, S.; Singh, S. K.; Rajaraman, G.; Shanmugam, M. Origin of SMM behaviour in an asymmetric Er(iii) Schiff base complex: a combined experimental and theoretical study. *Chem. Commun.* **2015**, *51*, 6137. (b) Upadhyay, A.; Singh, S. K.; Das, C.; Mondol, R.; Langley, S. K.; Murray, K. S.; Rajaraman, G.; Shanmugam, M. Enhancing the effective energy barrier of a Dy(iii)

DOI: 10.1021/acs.inorgchem.6b01831
Inorg. Chem. 2016, 55, 11201−11215

SMM using a bridged diamagnetic Zn(ii) ion. *Chem. Commun.* **2014**, *50*, 8838. (c) Singh, S. K.; Gupta, T.; Rajaraman, G. Magnetic Anisotropy and Mechanism of Magnetic Relaxation in Er(III) Single-Ion Magnets. *Inorg. Chem.* **2014**, *53*, 10835. (d) Singh, S. K.; Gupta, T.; Shanmugam, M.; Rajaraman, G. Unprecedented Magnetic Relaxation via Fourth Excited State in Low-Coordinate Lanthanide Single-ion Magnets: A Theoretical Perspective. *Chem. Commun.* **2014**, *50*, 15513. (e) Gupta, T.; Rajaraman, G. How strongly are the magnetic anisotropy and coordination numbers correlated in lanthanide based molecular magnets? *J. Chem. Sci.* **2014**, *126*, 1569. (f) Costes, J.-P.; Titos-Padilla, S.; Oyarzabal, I.; Gupta, T.; Duhayon, C.; Rajaraman, G.; Colacio, E. Analysis of the Role of Peripheral Ligands Coordinated to ZnII in Enhancing the Energy Barrier in Luminescent Linear Trinuclear Zn-Dy-Zn Single-Molecule Magnets. *Chem. - Eur. J.* **2015**, *21*, 15785. (g) Das, C.; Vaidya, S.; Gupta, T.; Frost, J. M.; Righi, M.; Brechin, E. K.; Affronte, M.; Rajaraman, G.; Shanmugam, M. *Chem. - Eur. J.* **2015**, *21*, 15639. (h) Costes, J. P.; Titos-Padilla, S.; Oyarzabal, I.; Gupta, T.; Duhayon, C.; Rajaraman, G.; Colacio, E. Effect of Ligand Substitution around the DyIII on the SMM Properties of Dual-Luminescent Zn−Dy and Zn−Dy−Zn Complexes with Large Anisotropy Energy Barriers: A Combined Theoretical and Experimental Magnetostructural Study. *Inorg. Chem.* **2016**, *55*, 4428.

(25) (a) Lin, S.-Y.; Wernsdorfer, W.; Ungur, L.; Powell, A. K.; Guo, Y.-N.; Tang, J.; Zhao, L.; Chibotaru, L. F.; Zhang, H.-J. Coupling Dy3 Triangles to Maximize the Toroidal Moment. *Angew. Chem., Int. Ed.* **2012**, *51*, 12767. (b) Langley, S. K.; Ungur, L.; Chilton, N. F.; Moubaraki, B.; Chibotaru, L. F.; Murray, K. S. Structure, Magnetism and Theory of a Family of Nonanuclear CuII5LnIII4−Triethanolamine Clusters Displaying Single-Molecule Magnet Behaviour. *Chem. - Eur. J.* **2011**, *17*, 9209.

(26) (a) Aquilante, F.; De Vico, L.; Ferre, N.; Ghigo, G.; Malmqvist, P. A.; Neogrady, P.; Pedersen, T. B.; Pitonak, M.; Reiher, M.; Roos, B. O.; Serrano-Andres, L.; Urban, M.; Veryazov, V.; Lindh, R. Software News and Update MOLCAS 7: The Next Generation. *J. Comput. Chem.* **2010**, *31*, 224. (b) Duncan, J. A. Molcas 7.2. *J. Am. Chem. Soc.* **2009**, *131*, 2416. (c) Swerts, B.; Chibotaru, L. F.; Lindh, R.; Seijo, L.; Barandiaran, Z.; Clima, S.; Pierloot, K.; Hendrickx, M. F. A. Embedding fragment ab initio model potentials in CASSCF/CASPT2 calculations of doped solids: Implementation and applications. *J. Chem. Theory Comput.* **2008**, *4*, 586. (d) Veryazov, V.; Widmark, P. O.; Serrano-Andres, L.; Lindh, R.; Roos, B. O. 2MOLCAS as a development platform for quantum chemistry software. *Int. J. Quantum Chem.* **2004**, *100*, 626. (e) Karlstrom, G.; Lindh, R.; Malmqvist, P. A.; Roos, B. O.; Ryde, U.; Veryazov, V.; Widmark, P. O.; Cossi, M.; Schimmelpfennig, B.; Neogrady, P.; Seijo, L. MOLCAS: a program package for computational chemistry. *Comput. Mater. Sci.* **2003**, *28*, 222.

(27) Malmqvist, P. A.; Roos, B. O.; Schimmelpfennig, B. The restricted active space (RAS) state interaction approach with spin-orbit coupling. *Chem. Phys. Lett.* **2002**, *357*, 230.

(28) (a) Ungur, L.; Lin, S.-Y.; Tang, J.; Chibotaru, L. F. Single-molecule toroics in Ising-type lanthanide molecular clusters. *Chem. Soc. Rev.* **2014**, *43*, 6894. (b) Pedersen, K. S.; Ungur, L.; Sigrist, M.; Sundt, A.; Schau-Magnussen, M.; Vieru, V.; Mutka, H.; Rols, S.; Weihe, H.; Waldmann, O.; Chibotaru, L. F.; Bendix, J.; Dreiser, J. Modifying the properties of 4f single-ion magnets by peripheral ligand functionalisation. *Chem. Sci.* **2014**, *5*, 1650. (c) Jiang, S.-D.; Wang, B.-W.; Gao, S. Springer: Berlin, 2014; pp 1.

(29) (a) Huang, X.-C.; Vieru, V.; Chibotaru, L. F.; Wernsdorfer, W.; Jiang, S.-D.; Wang, X.-Y. Determination of magnetic anisotropy in a multinuclear TbIII-based single-molecule magnet. *Chem. Commun.* **2015**, *51*, 10373. (b) Lines, M. E. Orbital Angular Momentum in the Theory of Paramagnetic Clusters. *J. Chem. Phys.* **1971**, *55*, 2977.

(30) Neese, F. The ORCA program system. *WIREs Comput. Mol. Sci.* **2012**, *2*, 73.

(31) Noodleman, L. Valence Bond Description of Anti-Ferromagnetic Coupling in Transition-Metal Dimers. *J. Chem. Phys.* **1981**, *74*, 5737.

(32) (a) Pantazis, D. A.; Neese, F. All-Electron Scalar Relativistic Basis Sets for the Lanthanides. *J. Chem. Theory Comput.* **2009**, *5*, 2229. (b) van Lenthe, E.; Baerends, E. J.; Snijders, J. G. Relativistic Regular 2-Component Hamiltonians. *J. Chem. Phys.* **1993**, *99*, 4597. (c) Douglas, M.; Kroll, N. M. Quantum Electrodynamical Corrections to Fine-Structure of Helium. *Ann. Phys.* **1974**, *82*, 89.

(33) (a) Singh, S. K.; Rajeshkumar, T.; Chandrasekhar, V.; Rajaraman, G. Theoretical studies on {3d-Gd} and {3d-Gd-3d} complexes: Effect of metal substitution on the effective exchange interaction. *Polyhedron* **2013**, *66*, 81. (b) Singh, S. K.; Rajaraman, G. Decisive interactions that determine ferro/antiferromagnetic coupling in {3d-4f} pairs: a case study on dinuclear {V(IV)-Gd(III)} complexes. *Dalton Trans.* **2013**, *42*, 3623. (c) Singh, S. K.; Pedersen, K. S.; Sigrist, M.; Thuesen, C. A.; Schau-Magnussen, M.; Mutka, H.; Piligkos, S.; Weihe, H.; Rajaraman, G.; Bendix, J. Angular dependence of the exchange interaction in fluoride-bridged GdIII-CrIII complexes. *Chem. Commun.* **2013**, *49*, 5583. (d) Rajeshkumar, T.; Singh, S. K.; Rajaraman, G. A computational perspective on magnetic coupling, magneto-structural correlations and magneto-caloric effect of a ferromagnetically coupled {Gd-III-Gd-III} pair. *Polyhedron* **2013**, *52*, 1299. (e) Singh, S. K.; Tibrewal, N. K.; Rajaraman, G. Density functional studies on dinuclear {NiIIGdIII} and trinuclear {NiIIGdIII-NiII} complexes: magnetic exchange and magneto-structural maps. *Dalton Trans.* **2011**, *40*, 10897. (f) Rajaraman, G.; Totti, F.; Bencini, A.; Caneschi, A.; Sessoli, R.; Gatteschi, D. Density functional studies on the exchange interaction of a dinuclear Gd(III)-Cu(II) complex: method assessment, magnetic coupling mechanism and magneto-structural correlations. *Dalton Trans.* **2009**, 3153. (g) Cremades, E.; Gomez-Coca, S.; Aravena, D.; Alvarez, S.; Ruiz, E. Theoretical Study of Exchange Coupling in 3d-Gd Complexes: Large Magnetocaloric Effect Systems. *J. Am. Chem. Soc.* **2012**, *134*, 10532. (h) Cirera, J.; Ruiz, E. Exchange coupling in (CuGdIII)-Gd-II dinuclear complexes: A theoretical perspective. *C. R. Chim.* **2008**, *11*, 1227.

(34) (a) Oyarzabal, I.; Ruiz, J.; Seco, J. M.; Evangelisti, M.; Camón, A.; Ruiz, E.; Aravena, D.; Colacio, E. Rational Electrostatic Design of Easy-Axis Magnetic Anisotropy in a ZnII−DyIII−ZnII Single-Molecule Magnet with a High Energy Barrier. *Chem. - Eur. J.* **2014**, *20*, 14262. (b) Zhang, P.; Zhang, L.; Lin, S.-Y.; Tang, J. Tetranuclear [MDy]2 Compounds and Their Dinuclear [MDy] (M = Zn/Cu) Building Units: Their Assembly, Structures, and Magnetic Properties. *Inorg. Chem.* **2013**, *52*, 6595. (c) Yu, W.-R.; Lee, G.-H.; Yang, E.-C. Systematic studies of the structures and magnetic properties for a family of cubane complexes with the formula: [M2Ln2] (Ln = Dy, Gd; M = Ni, Zn) and [Ni2Y2]. *Dalton Trans.* **2013**, *42*, 3941. (d) Towatari, M.; Nishi, K.; Fujinami, T.; Matsumoto, N.; Sunatsuki, Y.; Kojima, M.; Mochida, N.; Ishida, T.; Re, N.; Mrozinski, J. Syntheses, Structures, and Magnetic Properties of Acetato- and Diphenolato-Bridged 3d−4f Binuclear Complexes [M(3-MeOsaltn) (MeOH)x(ac)Ln(hfac)2] (M = ZnII, CuII, NiII, CoII; Ln = LaIII, GdIII, TbIII, DyIII; 3-MeOsaltn = N,N′-Bis(3-methoxy-2-oxybenzylidene)-1,3-propanediaminato; ac = Acetato; hfac = Hexafluoroacetylacetonato; x = 0 or 1). *Inorg. Chem.* **2013**, *52*, 6160. (e) Titos-Padilla, S.; Ruiz, J.; Herrera, J. M.; Brechin, E. K.; Wersndorfer, W.; Lloret, F.; Colacio, E. Dilution-Triggered SMM Behavior under Zero Field in a Luminescent Zn2Dy2 Tetranuclear Complex Incorporating Carbonato-Bridging Ligands Derived from Atmospheric CO2 Fixation. *Inorg. Chem.* **2013**, *52*, 9620. (f) Palacios, M. A.; Titos-Padilla, S.; Ruiz, J.; Herrera, J. M.; Pope, S. J. A.; Brechin, E. K.; Colacio, E. Bifunctional ZnIILnIII Dinuclear Complexes Combining Field Induced SMM Behavior and Luminescence: Enhanced NIR Lanthanide Emission by 9-Anthracene Carboxylate Bridging Ligands. *Inorg. Chem.* **2014**, *53*, 1465. (g) Ehama, K.; Ohmichi, Y.; Sakamoto, S.; Fujinami, T.; Matsumoto, N.; Mochida, N.; Ishida, T.; Sunatsuki, Y.; Tsuchimoto, M.; Re, N. Synthesis, Structure, Luminescent, and Magnetic Properties of Carbonato-Bridged ZnII2LnIII2 Complexes [(μ4-CO3)2-{ZnIILnLnIII(NO3)}2] (LnIII = GdIII, TbIII, DyIII; L1 = N,N′-Bis(3-methoxy-2-oxybenzylidene)-1,3-propanediaminato, L2 = N,N′-Bis(3-ethoxy-2-oxybenzylidene)-1,3-propanediaminato). *Inorg. Chem.* **2013**, *52*, 12828. (h) Maeda, M.; Hino, S.; Yamashita, K.; Kataoka, Y.;

DOI: 10.1021/acs.inorgchem.6b01831
Inorg. Chem. 2016, 55, 11201−11215

Nakano, M.; Yamamura, T.; Kajiwara, T. Correlation between slow magnetic relaxation and the coordination structures of a family of linear trinuclear Zn(ii)-Ln(iii)-Zn(ii) complexes (Ln = Tb, Dy, Ho, Er, Tm and Yb). *Dalton Trans.* **2012**, *41*, 13640. (i) Burrow, C. E.; Burchell, T. J.; Lin, P. H.; Habib, F.; Wernsdorfer, W.; Clerac, R.; Murugesu, M. Salen-Based [Zn(2)Ln(3)] Complexes with Fluorescence and Single-Molecule-Magnet Properties. *Inorg. Chem.* **2009**, *48*, 8051.

(35) (a) Ungur, L.; Langley, S. K.; Hooper, T. N.; Moubaraki, B.; Brechin, E. K.; Murray, K. S.; Chibotaru, L. F. Net Toroidal Magnetic Moment in the Ground State of a {Dy6}-Triethanolamine Ring. *J. Am. Chem. Soc.* **2012**, *134*, 18554. (b) Bhunia, A.; Gamer, M. T.; Ungur, L.; Chibotaru, L. F.; Powell, A. K.; Lan, Y.; Roesky, P. W.; Menges, F.; Riehn, C.; Niedner-Schatteburg, G. From a Dy(III) Single Molecule Magnet (SMM) to a Ferromagnetic [Mn(II)Dy(III)Mn(II)] Trinuclear Complex. *Inorg. Chem.* **2012**, *51*, 9589.

(36) Peng, G.; Mereacre, V.; Kostakis, G. E.; Wolny, J. A.; Schünemann, V.; Powell, A. K. Enhancement of Spin Relaxation in an FeDy2Fe Coordination Cluster by Magnetic Fields. *Chem. - Eur. J.* **2014**, *20*, 12381.

(37) Paulovic, J.; Cimpoesu, F.; Ferbinteanu, M.; Hirao, K. Mechanism of ferromagnetic coupling in copper(II)-gadolinium(II) complexes. *J. Am. Chem. Soc.* **2004**, *126*, 3321.

(38) Fohlmeister, L.; Vignesh, K. R.; Winter, F.; Moubaraki, B.; Rajaraman, G.; Pottgen, R.; Murray, K. S.; Jones, C. Neutral diiron(iii) complexes with Fe2([small mu]-E)2 (E = O, S, Se) core structures: reactivity of an iron(i) dimer towards chalcogens. *Dalton Trans.* **2015**, *44*, 1700.

(39) Tuna, F.; Smith, C. A.; Bodensteiner, M.; Ungur, L.; Chibotaru, L. F.; McInnes, E. J. L.; Winpenny, R. E. P.; Collison, D.; Layfield, R. A. A High Anisotropy Barrier in a Sulfur-Bridged Organodysprosium Single-Molecule Magnet. *Angew. Chem., Int. Ed.* **2012**, *51*, 6976.

(40) Costes, J.-P.; Dahan, F.; Dupuis, A. Influence of Anionic Ligands (X) on the Nature and Magnetic Properties of Dinuclear LCuGdX3·nH2O Complexes (LH2 Standing for Tetradentate Schiff Base Ligands Deriving from 2-Hydroxy-3-methoxybenzaldehyde and X Being Cl, N3C2, and CF3COO). *Inorg. Chem.* **2000**, *39*, 165.

(41) Llunell, S. A. M.; Casanova, D.; Cirera, J.; Alemany, P. *SHAPE version 2.1*, Bareclona, 2010.

(42) Pedersen, K. S.; Dreiser, J.; Weihe, H.; Sibille, R.; Johannesen, H. V.; Sørensen, M. A.; Nielsen, B. E.; Sigrist, M.; Mutka, H.; Rols, S.; Bendix, J.; Piligkos, S. Design of Single-Molecule Magnets: Insufficiency of the Anisotropy Barrier as the Sole Criterion. *Inorg. Chem.* **2015**, *54*, 7600.

(43) (a) Lucaccini, E.; Sorace, L.; Perfetti, M.; Costes, J.-P.; Sessoli, R. Beyond the anisotropy barrier: slow relaxation of the magnetization in both easy-axis and easy-plane Ln(trensal) complexes. *Chem. Commun.* **2014**, *50*, 1648. (b) Colacio, E.; Ruiz, J.; Ruiz, E.; Cremades, E.; Krzystek, J.; Carretta, S.; Cano, J.; Guidi, T.; Wernsdorfer, W.; Brechin, E. K. Slow Magnetic Relaxation in a CoII−YIII Single-Ion Magnet with Positive Axial Zero-Field Splitting. *Angew. Chem., Int. Ed.* **2013**, *52*, 9130.

(44) Ungur, L.; Chibotaru, L. F. *POLY_ANISO program*; KU Leuven: Leuven, Belgium, 2007.

(45) Ungur, L.; Chibotaru, L. F. *SINGLE_ANISO module in MOLCAS*; KU Leuven: Leuven, Belgium, 2007; http://www.molcas.org/documentation/manual/node95.html.

(46) Ida, Y.; Ghosh, S.; Ghosh, A.; Nojiri, H.; Ishida, T. Strong Ferromagnetic Exchange Interactions in Hinge-like Dy(O2Cu)2 Complexes Involving Double Oxygen Bridges. *Inorg. Chem.* **2015**, *54*, 9543.

(47) (a) Andruh, M.; Ramade, I.; Codjovi, E.; Guillou, O.; Kahn, O.; Trombe, J. C. Crystal structure and magnetic properties of [Ln2Cu4] hexanuclear clusters (where Ln = trivalent lanthanide). Mechanism of the gadolinium(III)-copper(II) magnetic interaction. *J. Am. Chem. Soc.* **1993**, *115*, 1822. (b) Benelli, C.; Caneschi, A.; Gatteschi, D.; Guillou, O.; Pardi, L. Synthesis, Crystal-Structure, and Magnetic-Properties of Tetranuclear Complexes Containing Exchange-Coupled Gd2cu2, Dy2cu2 Species. *Inorg. Chem.* **1990**, *29*, 1750. (c) Benelli, C.; Caneschi, A.; Fabretti, A. C.; Gatteschi, D.; Pardi, L. Ferromagnetic Coupling of Gadolinium(Iii) Ions and Nitronyl Nitroxide Radicals in an Essentially Isotropic Way. *Inorg. Chem.* **1990**, *29*, 4153. (d) Kollmar, C.; Kahn, O. *Acc. Chem. Res.* **1993**, *26*, 259. (e) Ramade, I.; Kahn, O.; Jeannin, Y.; Robert, F. Design and Magnetic Properties of a Magnetically Isolated GdIIICuII Pair. Crystal Structures of [Gd(hfa)-3Cu(salen)], [Y(hfa)3Cu(salen)], [Gd(hfa)3Cu(salen) (Meim)], and [La(hfa)3(H2O)Cu(salen)] [hfa = Hexafluoroacetylacetonato, salen = N,N′-Ethylenebis(salicylideneaminato), Meim = 1-Methylimidazole]. *Inorg. Chem.* **1997**, *36*, 930. (f) Guillou, O.; Bergerat, P.; Kahn, O.; Bakalbassis, E.; Boubekeur, K.; Batail, P.; Guillot, M. Ferromagnetically coupled gadolinium(III)copper(II) molecular material. *Inorg. Chem.* **1992**, *31*, 110.

(48) Jacobson, P.; Herden, T.; Muenks, M.; Laskin, G.; Brovko, O.; Stepanyuk, V.; Ternes, M.; Kern, K. Quantum engineering of spin and anisotropy in magnetic molecular junctions. *Nat. Commun.* **2015**, *6*, 8536.

(49) (a) Liu, J.-L.; Wu, J.-Y.; Huang, G.-Z.; Chen, Y.-C.; Jia, J.-H.; Ungur, L.; Chibotaru, L. F.; Chen, X.-M.; Tong, M.-L. Desolvation-Driven 100-Fold Slow-down of Tunneling Relaxation Rate in Co(II)-Dy(III) Single-Molecule Magnets through a Single-Crystal-to-Single-Crystal Process. *Sci. Rep.* **2015**, *5*, 16621. (b) Rechkemmer, Y.; Fischer, J. E.; Marx, R.; Dörfel, M.; Neugebauer, P.; Horvath, S.; Gysler, M.; Brock-Nannestad, T.; Frey, W.; Reid, M. F.; van Slageren, J. Comprehensive Spectroscopic Determination of the Crystal Field Splitting in an Erbium Single-Ion Magnet. *J. Am. Chem. Soc.* **2015**, *137*, 13114. (c) Marx, R.; Moro, F.; Dorfel, M.; Ungur, L.; Waters, M.; Jiang, S. D.; Orlita, M.; Taylor, J.; Frey, W.; Chibotaru, L. F.; van Slageren, J. Spectroscopic determination of crystal field splittings in lanthanide double deckers. *Chem. Sci.* **2014**, *5*, 3287.

(50) (a) Comba, P.; Großhauser, M.; Klingeler, R.; Koo, C.; Lan, Y.; Müller, D.; Park, J.; Powell, A.; Riley, M. J.; Wadepohl, H. Magnetic Interactions in a Series of Homodinuclear Lanthanide Complexes. *Inorg. Chem.* **2015**, *54*, 11247. (b) Cornia, A.; Gatteschi, D.; Sessoli, R. New experimental techniques for magnetic anisotropy in molecular materials. *Coord. Chem. Rev.* **2001**, *219*, 573 and references therein. (c) Rawat, N.; Pan, Z.; Lamarche, C. J.; Wetherby, A.; Waterman, R.; Tokumoto, T.; Cherian, J. G.; Headrick, R. L.; McGill, S. A.; Furis, M. I. Spin Exchange Interaction in Substituted Copper Phthalocyanine Crystalline Thin Films. *Sci. Rep.* **2015**, *5*, 16536.

(51) Gupta, S. K.; Rajeshkumar, T.; Rajaraman, G.; Murugavel, R. An Air-Stable Dy(III) Single-Ion Magnet with High Anisotropy Barrier and Blocking Temperature. *Chem. Sci.* **2016**, *7*, 5181.

(52) (a) Feltham, H. L. C.; Clérac, R.; Ungur, L.; Chibotaru, L. F.; Powell, A. K.; Brooker, S. By Design: A Macrocyclic 3d−4f Single-Molecule Magnet with Quantifiable Zero-Field Slow Relaxation of Magnetization. *Inorg. Chem.* **2013**, *52*, 3236. (b) Huang, X.-C.; Vieru, V.; Chibotaru, L. F.; Wernsdorfer, W.; Jiang, S.-D.; Wang, X.-Y. Determination of magnetic anisotropy in a multinuclear TbIII-based single-molecule magnet. *Chem. Commun.* **2015**, *51*, 10373.

(53) (a) Vieru, V.; Iwahara, N.; Ungur, L.; Chibotaru, L. F. Giant Exchange Interaction in Mixed Lanthanides. *Sci. Rep.* **2016**, *6*, 24046. (b) Vieru, V.; Chibotaru, L. F. Redox Switches for Single-Molecule Magnet Activity: An Ab Initio Insight. *Chem. - Eur. J.* **2016**, *22*, 5309. (c) Iwahara, N.; Chibotaru, L. F. New mechanism of kinetic exchange interaction induced by strong magnetic anisotropy. *Sci. Rep.* **2016**, *6*, 24743. (d) Pugh, T.; Vieru, V.; Chibotaru, L. F.; Layfield, R. A. Magneto-structural correlations in arsenic- and selenium-ligated dysprosium single-molecule magnets. *Chem. Sci.* **2016**, *7*, 2128. (e) Chibotaru, L. V.; Iwahara, N. Ising exchange interaction in lanthanides and actinides. *New J. Phys.* **2015**, *17*, 103028. (f) Bender, M.; Comba, P.; Demeshko, S.; Großhauser, M.; Müller, D.; Wadepohl, H. Theoretically predicted and experimentally observed relaxation pathways of two heterodinuclear 3d-4f complexes. *Z. Anorg. Allg. Chem.* **2015**, *641*, 2291.

DOI: 10.1021/acs.inorgchem.6b01831
Inorg. Chem. 2016, 55, 11201−11215